Trace expressions and associated limits for equilibrium Casimir torque

Benjamin Strekha,[1] Matthias Krüger,[2] and Alejandro W. Rodriguez[1]
[1]*Department of Electrical and Computer Engineering, Princeton University, Princeton, New Jersey 08544, USA*
[2]*Institute for Theoretical Physics, Georg-August-Universität Göttingen, 37073 Göttingen, Germany*

(Received 31 October 2023; accepted 4 January 2024; published 22 January 2024)

We exploit fluctuational electrodynamics to present trace expressions for the torque experienced by arbitrary objects in a passive, nonabsorbing, rotationally invariant background environment. We present trace expressions for equilibrium Casimir torque which complement recently derived nonequilibrium torque expressions and explicate their relation to the Casimir free energy. We then use the derived trace expressions to calculate, via Lagrange duality, semianalytic structure-agnostic bounds on the Casimir torque between an anisotropic (reciprocal or nonreciprocal) dipolar particle and a macroscopic body composed of a local isotropic electric susceptibility, separated by vacuum.

DOI: 10.1103/PhysRevA.109.012813

I. INTRODUCTION

Fluctuation phenomena have been successfully studied and measured in the past few decades [1,2]. Experiments involving a sphere-plate setup have measured radiative heat transfer [3,4], an attractive Casimir force [5,6], and a long-range repulsive Casimir force [7]. Casimir torque, on the other hand, has been less studied to date. In anisotropic media or systems exhibiting chirality, thermal fluctuations can also cause objects to exchange net angular momentum with their environments or other nearby objects, resulting in a predicted net torque [8–13]. Several theoretical proposals to detect the Casimir torque include birefringent plates [14], anisotropic nanostructures [15,16], and liquid crystals [17]. The challenge in each system for detection stems from the weakness of the effect and the requirement of ultrasensitive measurements; a larger effect requires the ability to place objects at a small separation. The prediction of a Casimir torque was eventually confirmed experimentally between a liquid crystal and a solid birefringent crystal where, to ensure that the two surfaces were parallel (a problem less relevant for sphere-plate setups), the vacuum gap was replaced by an isotropic material to act as a spacer layer [18]. The measurement of Casimir torque between two objects (a nanorod levitated by a linearly polarized optical tweezer near a birefringent plate) with a vacuum gap was proposed in Ref. [19] but has not yet been realized, although recent experiments [20,21] with an optically levitated nanodumbbell or nanosphere in vacuum demonstrated a torque detection sensitivity on the order of 10^{-27} N m Hz$^{-1/2}$, demonstrating progress towards detecting a Casimir torque in a setup involving a dipolar particle near a macroscopic body, separated by vacuum.

In calculating equilibrium Casimir forces on a rigid body, it is common to start with a Casimir free energy and then take a negative derivative with respect to the position of the body to get a force [22–24]. The equilibrium Casimir torque is expected to be a rotational derivative of the Casimir free energy and indeed was calculated in the above-cited works from the Casimir free energy. In this article we start from the general Lorentz force law and then use the mathematical framework of fluctuational electrodynamics [25,26] and scattering theory [22] to derive trace expressions for the thermal Casimir forces and torques experienced by a set of objects in thermal equilibrium which elucidate in a unified framework the precise relationship of force and torque to the Casimir free energy. In particular, the torque is confirmed to be a rotational derivative of the Casimir free energy but, since photons are spin-1 particles, the rotation is an angular rotation of the center of mass of the body plus a rotation of the vector components of the scattering operator.

As an application of the derived torque expressions, we calculate bounds on the Casimir torque on an anisotropic dipolar particle from neighboring objects. There is the interesting question of whether Casimir torques must be weak. Reference [27] predicts a giant torque per unit area for two metallic one-dimensional gratings rotated by a small angle, with diverging torque near zero rotation angle as the system sizes diverge. How large can the Casimir torque be if one object is restricted to be finite in spatial extent or even dipolar? As the ability to manipulate mechanical devices of increasingly smaller scales continues to increase, so too will the interest in exploiting fluctuation phenomena such as laser shot noise and the Casimir effect as a mechanism of control in micromachines [28–30]. The natural question of which geometry leads to maximum torque can be probed via large-scale optimization but cannot in general provide guarantees of global optimality [31,32]. Further understanding, e.g., of quantitative bounds and scaling behavior, can be gained by applying a recent framework based on Lagrange duality to compute shape-independent bounds [13,33–37]. In particular, Ref. [36] presents bounds on the surface-perpendicular Casimir force on a dipole above a half-space design domain and the authors remark that similar methods can be used for bounds on Casimir torques by taking a derivative of the dipolar basis functions with respect to a rotation angle. Naive manipulations and rotational derivatives will yield incorrect results by missing "spin" contributions. Our derived expressions with an explicit appearance of a total angular momentum operator $\hat{\mathbf{J}}$ allow for a more lucid analysis of torque phenomena.

II. EQUILIBRIUM CASIMIR EFFECTS

As explained in detail in Refs. [13,38–41], starting from the Lorentz force law, one can show that the thermally averaged ($\langle\cdots\rangle_T$) rate of absorption associated with an observable $\hat{\Theta}$ is given by

$$\langle\hat{\Theta}\rangle_T = -\text{Im}\int_{-\infty}^{\infty} d\omega \frac{1}{\hbar c^2\mu_0}\text{Tr}|_{V_{\text{body}}}(\hat{\Theta}\mathbb{C}\mathbb{G}_0^{-1\dagger}), \quad (1)$$

where substituting $\hbar\omega\mathbb{I}$, $\hat{\mathbf{p}}$, and $\hat{\mathbf{J}}$ for $\hat{\Theta}$ above yields the absorbed power, force, and torque on the body, respectively. Here $\hat{\mathbf{p}} \equiv -i\hbar\nabla$ is the linear momentum operator, $\hat{\mathbf{J}} \equiv \hat{\mathbf{L}} + \hat{\mathbf{S}}$ is the total angular momentum operator, $\hat{\mathbf{L}} \equiv \mathbf{r}\times\hat{\mathbf{p}} = -i\hbar\mathbf{r}\times\nabla$, and

$$\hat{\mathbf{S}} \equiv -i\hbar\left\{\begin{bmatrix}0&0&0\\0&0&1\\0&-1&0\end{bmatrix},\begin{bmatrix}0&0&-1\\0&0&0\\1&0&0\end{bmatrix},\begin{bmatrix}0&1&0\\-1&0&0\\0&0&0\end{bmatrix}\right\} \quad (2)$$

are orbital and spin angular momentum operators [42], respectively, defined in the Cartesian basis and compactly summarized by $(\hat{S}_a)_{bc} = -i\hbar\epsilon_{abc}$. The notation $|_{V_{\text{body}}}$ denotes that the outermost indices of the operator are traced over positions in the body, while all others are over all space, and a trace over the vector components of the dyadics, that is, $\text{Tr}|_V(\mathbb{A}\mathbb{B}) = \sum_{ab}\int_{\mathbf{r}\in V}\int_{\mathbf{s}\in\mathbb{R}^3} d^3\mathbf{r}\, d^3\mathbf{s}\,\mathbb{A}_{ab}(\mathbf{r},\mathbf{s})\mathbb{B}_{ba}(\mathbf{s},\mathbf{r})$ or, alternatively, $\text{Tr}|_V[(\cdots)] = \text{Tr}[\mathbb{P}(V)(\cdots)]$, where $\mathbb{P}(V)$ is a projection operator into the spatial volume V. The operator $\mathbb{G}_0$ represents the background Green's function, which in vacuum satisfies $(\nabla\times\nabla\times -\frac{\omega^2}{c^2}\mathbb{I})\mathbb{G}_0(\mathbf{r},\mathbf{r}') = \frac{\omega^2}{c^2}\mathbb{I}\delta^{(3)}(\mathbf{r}-\mathbf{r}')$. For systems in thermal equilibrium the field-field correlations satisfy $\mathbb{C}_{ij}^{\text{eq}}(T,\omega,\omega';\mathbf{r},\mathbf{r}') \equiv \langle E_i(\mathbf{r},\omega)E_j^*(\mathbf{r}',\omega')\rangle_T = \frac{\hbar}{2\pi\epsilon_0}\coth(\frac{\hbar\omega}{2k_BT})\delta(\omega-\omega')\mathbb{G}_{ij}^{\mathsf{A}}(\omega;\mathbf{r},\mathbf{r}')$, where $\mathbb{G}$ is the Green's function of the system, defined by $[\nabla\times\nabla\times -\frac{\omega^2}{c^2}(\mathbb{V}+\mathbb{I})]\mathbb{G}(\mathbf{r},\mathbf{r}') = \frac{\omega^2}{c^2}\mathbb{I}\delta^{(3)}(\mathbf{r}-\mathbf{r}')$, where $\mathbb{V} = (\epsilon-\mathbb{I}) + \frac{c^2}{\omega^2}\nabla\times(\mathbb{I}-\mu^{-1})\nabla\times$ is the potential or generalized susceptibility introduced by the objects [43]. The superscript A on an operator $\hat{\Theta}$ denotes a Hermitian operator which contains the anti-Hermitian part of $\hat{\Theta}$, defined by $\hat{\Theta}^{\mathsf{A}} \equiv \frac{1}{2i}(\hat{\Theta}-\hat{\Theta}^\dagger)$, where the dagger denotes conjugate transpose. In our notation, $\hat{\Theta}_{ab}^\dagger(\mathbf{x},\mathbf{y}) = \hat{\Theta}_{ba}(\mathbf{y},\mathbf{x})^*$, treating the vector component and spatial coordinate as an index pair.

For a single body, the Green's function satisfies $\mathbb{G} = \mathbb{G}_0 + \mathbb{G}_0\mathbb{T}\mathbb{G}_0$, where we have introduced the scattering $\mathbb{T}$ operator which transforms incident fields into induced currents in the body and is formally defined by the relation $\mathbb{T} = \mathbb{V}(\mathbb{I}-\mathbb{G}_0\mathbb{V})^{-1}$ [38]. Since $\mathbb{T}$ vanishes unless both spatial arguments are within the body, the integral can be extended over all space to get a trace expression

$$\langle\hat{\Theta}\rangle_T^{\text{eq}} = \text{Re}\int_{-\infty}^{\infty}\frac{d\omega}{4\pi}\coth\left(\frac{\hbar\omega}{2k_BT}\right)\text{Tr}[\hat{\Theta}(\mathbb{G}_0\mathbb{T}-\mathbb{G}_0^\dagger\mathbb{T}^\dagger)]. \quad (3)$$

However, $\text{Re}\,\text{Tr}[\hat{\Theta}(\mathbb{G}_0\mathbb{T}-\mathbb{G}_0^\dagger\mathbb{T}^\dagger)] = 0$ independent of $\mathbb{V}$ (reciprocal or nonreciprocal), so the net power absorption, force, and torque on an isolated object in equilibrium are identically zero, as expected.

Consider next the case of two or more bodies. The Green's function is found by starting with object 1 in isolation with $\mathbb{G}_1 = (1+\mathbb{G}_0\mathbb{T}_1)\mathbb{G}_0$ and then inserting the rest of the objects to get $\mathbb{G} = (1+\mathbb{G}_0\mathbb{T}_{\bar{1}})\frac{1}{1-\mathbb{G}_0\mathbb{T}_1\mathbb{G}_0\mathbb{T}_{\bar{1}}}(1+\mathbb{G}_0\mathbb{T}_1)\mathbb{G}_0$, where $\mathbb{T}_{\bar{1}}$ denotes the scattering operator of all objects excluding object 1 [38]. Changing the order of object insertion implies that the same equation with the indices swapped $1\leftrightarrow\bar{1}$ holds as well. Using these expressions for the Green's function in the equilibrium field-field correlation dyadic $\mathbb{C}^{\text{eq}}$ in Eq. (1), we find that the thermally averaged torques on the objects are (intermediate steps are provided in Appendix A)

$$\boldsymbol{\tau}^{(\alpha,\text{eq})}(T) = \text{Re}\frac{1}{\pi}\int_0^\infty d\omega\left[n(\omega,T)+\frac{1}{2}\right] \times \text{Tr}\left(\frac{1}{1-\mathbb{G}_0\mathbb{T}_\alpha\mathbb{G}_0\mathbb{T}_{\bar{\alpha}}}\mathbb{G}_0(\mathbb{T}_\alpha\hat{\mathbf{J}}-\hat{\mathbf{J}}\mathbb{T}_\alpha)\mathbb{G}_0\mathbb{T}_{\bar{\alpha}}\right), \quad (4)$$

where $n(\omega,T) = \frac{1}{\exp(\frac{\hbar\omega}{k_BT})-1}$ is the Bose-Einstein distribution function. The Tr symbol denotes a trace over the complete set of indices of the enclosed operators (for example, over all positions and polarization indices of the dipole sources). The switch from $\text{Tr}|_{V_\alpha}$ to Tr is possible since $\mathbb{C}^{\text{eq}}\mathbb{G}_0^{-1\dagger}$ has a $\mathbb{T}_\alpha$ or $\mathbb{T}_\alpha^\dagger$ with $\alpha = 1, \bar{1}$ as the leftmost or rightmost term in the expansion (Appendix A). Since $\mathbb{T}_\alpha$ vanishes if at least one of the spatial arguments is outside the volume V_α of body α, one can extend the spatial integration to be over the entire space, resulting in a trace expression. The above equations satisfy $\boldsymbol{\tau}^{(1,\text{eq})} = -\boldsymbol{\tau}^{(\bar{1},\text{eq})}$ (by the cyclicity of the trace along with resumming of $\frac{1}{1-\mathbb{G}_0\mathbb{T}_{\bar{1}}\mathbb{G}_0\mathbb{T}_1}$), as expected since the angular momentum transfer to the far field should cancel and detailed balance should hold. For the case of reciprocal materials, the expressions can be further simplified to

$$\boldsymbol{\tau}^{(\alpha,\text{eq})}(T) = \text{Re}\frac{2}{\pi}\int_0^\infty d\omega\left[n(\omega,T)+\frac{1}{2}\right] \times \text{Tr}\left(\hat{\mathbf{J}}\mathbb{G}_0\mathbb{T}_{\bar{\alpha}}\mathbb{G}_0\mathbb{T}_\alpha\frac{1}{1-\mathbb{G}_0\mathbb{T}_{\bar{\alpha}}\mathbb{G}_0\mathbb{T}_\alpha}\right). \quad (5)$$

The expressions for the equilibrium forces are identical but with $\hat{\mathbf{J}}\to\hat{\mathbf{p}}$, corresponding to a change in observable from rate of angular momentum absorption to rate of linear momentum absorption.

Equation (4) elucidates the relationship of the torque (and force) with the Casimir free energy $\mathcal{F}$, defined as

$$\mathcal{F} \equiv -\frac{\hbar}{\pi}\int_0^\infty d\omega\left[n(\omega,T)+\frac{1}{2}\right]\text{Im}\,\text{Tr}[\ln(1-\mathbb{G}_0\mathbb{T}_1\mathbb{G}_0\mathbb{T}_{\bar{1}})] \quad (6)$$

$$= -\frac{\hbar}{\pi}\int_0^\infty d\omega\left[n(\omega,T)+\frac{1}{2}\right]\text{Im}\ln[\det(1-\mathbb{G}_0\mathbb{T}_1\mathbb{G}_0\mathbb{T}_{\bar{1}})], \quad (7)$$

more directly than Eq. (5). Viewing the free energy $\mathcal{F}(\mathbb{T}_\alpha)$ as a function of $\mathbb{T}_\alpha = \mathbb{V}_\alpha(\mathbb{I} - \mathbb{G}_0\mathbb{V}_\alpha)^{-1}$, the equilibrium force and torque can be written as

$$\mathbf{F}^{(\alpha,\mathrm{eq})} = -\lim_{\Delta\mathbf{x}\to 0} \frac{\mathcal{F}\big(\exp\big(-\frac{i\Delta\mathbf{x}\cdot\hat{\mathbf{p}}}{\hbar}\big)\mathbb{T}_\alpha \exp\big(\frac{i\Delta\mathbf{x}\cdot\hat{\mathbf{p}}}{\hbar}\big)\big) - \mathcal{F}(\mathbb{T}_\alpha)}{\Delta\mathbf{x}}, \tag{8}$$

$$\boldsymbol{\tau}^{(\alpha,\mathrm{eq})} = -\lim_{\Delta\boldsymbol{\phi}\to 0} \frac{\mathcal{F}\big(\exp\big(-\frac{i\Delta\boldsymbol{\phi}\cdot\hat{\mathbf{J}}}{\hbar}\big)\mathbb{T}_\alpha \exp\big(\frac{i\Delta\boldsymbol{\phi}\cdot\hat{\mathbf{J}}}{\hbar}\big)\big) - \mathcal{F}(\mathbb{T}_\alpha)}{\Delta\boldsymbol{\phi}}, \tag{9}$$

as can be verified by taking the limit directly and recovering Eq. (4). Thus, the equilibrium force and torque on object α are changes in free energy due to a rigid translation and rotation of the scattering operator $\mathbb{T}_\alpha$ where, because photons are spin-1 particles, the relevant rotation operator $\exp(-\frac{i\Delta\boldsymbol{\phi}\cdot\hat{\mathbf{J}}}{\hbar})$ depends on $\hat{\mathbf{J}}$ and not $\hat{\mathbf{L}}$.

Assuming rigid bodies, the equilibrium Casimir force can be written more explicitly as a negative gradient of a free energy $\mathcal{F}$ (Appendix A of Ref. [38]). Concisely, assuming rigid bodies, then $\boldsymbol{\nabla}_{\mathcal{O}_1}\mathbb{T}_1 = \boldsymbol{\nabla}\mathbb{T}_1 - \mathbb{T}_1\boldsymbol{\nabla} = \frac{i}{\hbar}\hat{\mathbf{p}}\mathbb{T}_1 - \frac{i}{\hbar}\mathbb{T}_1\hat{\mathbf{p}}$, where $\boldsymbol{\nabla}_{\mathcal{O}_1}$ is a derivative with respect to the center-of-mass coordinate of object 1 so that

$$\mathbf{F}^{(1,\mathrm{eq})}(T) = \mathrm{Im}\frac{\hbar}{\pi}\int_0^\infty d\omega\Big[n(\omega,T) + \frac{1}{2}\Big] \times \mathrm{Tr}\boldsymbol{\nabla}_{\mathcal{O}_1}\ln(1 - \mathbb{G}_0\mathbb{T}_1\mathbb{G}_0\mathbb{T}_{\bar{1}}) \tag{10}$$

$$= -\boldsymbol{\nabla}_{\mathcal{O}_1}\mathcal{F}, \tag{11}$$

where the last line follows since $\boldsymbol{\nabla}_{\mathcal{O}_1}$ can be brought outside the trace. When calculating equilibrium torque, care must be taken to check if the torque is an angular derivative of the same free energy $\mathcal{F}$. In trying analogous steps for torque starting from Eq. (4) we find that the trace expressions cannot in general be rewritten as angular derivatives with respect to the center-of-mass coordinates of the rigid body, $-\mathbf{r}_{\mathcal{O}_1}\times\boldsymbol{\nabla}_{\mathcal{O}_1}\mathcal{F}$, due to the spin terms.

Some intuition can be gleaned from a dilute limit. In the Rytov formalism for fluctuational electrodynamics [25], the object is viewed as a collection of free dipoles which undergo fluctuations. In thermal equilibrium, the fluctuation-dissipation theorem states that the fluctuations are proportional to the polarizability tensor [43,44]. Consider two objects (viewed as two collections of fluctuating free dipoles) separated by a gap and call the free energy for a given initial arrangement $\mathcal{F}_i$. Then calculate the free energy when one of them is geometrically rotated by $\Delta\phi$ about the z axis but the polarizability or susceptibility tensor at the rotated spatial point is unchanged and call that final energy $\mathcal{F}_{f,L}$, that is, rotate the position of each dipole but not its orientation. Likewise, starting from the initial arrangement, keep the position of each dipole fixed but now instead rotate the orientation by $\Delta\phi$ around the z axis and call the resulting free energy $\mathcal{F}_{f,S}$. The torque on the object is given by $\lim_{\Delta\phi\to 0} -\frac{(\mathcal{F}_{f,L}-\mathcal{F}_i)+(\mathcal{F}_{f,S}-\mathcal{F}_i)}{\Delta\phi}$. Physically, both the spatial location and orientation of each free dipole are rotated during the rotation of an object, which is precisely what Eq. (9) states and Eq. (4) calculates.

As a word of caution, this simple interpretation breaks down past the dilute limit, in which case one can no longer view torque as due to a sum of pairwise interactions $\boldsymbol{\tau}^{(\alpha,\mathrm{eq})} \propto \mathrm{Tr}(\hat{\mathbf{J}}\mathbb{G}_0\mathbb{V}_{\tilde{\alpha}}\mathbb{G}_0\mathbb{V}_\alpha)$. In particular, if $\mathbb{V}_\alpha \to \exp(-\frac{i\Delta\boldsymbol{\phi}\cdot\hat{\mathbf{J}}}{\hbar})\mathbb{V}_\alpha\exp(\frac{i\Delta\boldsymbol{\phi}\cdot\hat{\mathbf{J}}}{\hbar})$, then $\mathbb{T}_\alpha \to \exp(-\frac{i\Delta\boldsymbol{\phi}\cdot\hat{\mathbf{J}}}{\hbar})\mathbb{T}_\alpha\exp(\frac{i\Delta\boldsymbol{\phi}\cdot\hat{\mathbf{J}}}{\hbar})$, as can be seen from the definition $\mathbb{T}_\alpha = \mathbb{V}_\alpha(1 - \mathbb{G}_0\mathbb{V}_\alpha)^{-1}$ and the fact that $\hat{\mathbf{J}}\mathbb{G}_0 = \mathbb{G}_0\hat{\mathbf{J}}$. Similar statements do *not* hold for the $\hat{\mathbf{S}}$ and $\hat{\mathbf{L}}$ operators since the spin and orbital angular momentum operators do not commute with $\mathbb{G}_0$. For example, the statement that if $\mathbb{V}_\alpha \to \exp(-\frac{i\Delta\boldsymbol{\phi}\cdot\hat{\mathbf{S}}}{\hbar})\mathbb{V}_\alpha\exp(\frac{i\Delta\boldsymbol{\phi}\cdot\hat{\mathbf{S}}}{\hbar})$ then $\mathbb{T}_\alpha \to \exp(-\frac{i\Delta\boldsymbol{\phi}\cdot\hat{\mathbf{S}}}{\hbar})\mathbb{T}_\alpha\exp(\frac{i\Delta\boldsymbol{\phi}\cdot\hat{\mathbf{S}}}{\hbar})$ is not generally true beyond the dilute limit. Instead, one would need to use $\mathbb{T}_\alpha \to \tilde{\mathbb{V}}_\alpha(1 - \mathbb{G}_0\tilde{\mathbb{V}}_\alpha)^{-1}$, where $\tilde{\mathbb{V}}_\alpha \equiv \exp(-\frac{i\Delta\boldsymbol{\phi}\cdot\hat{\mathbf{S}}}{\hbar})\mathbb{V}_\alpha\exp(\frac{i\Delta\boldsymbol{\phi}\cdot\hat{\mathbf{S}}}{\hbar})$.

III. BOUNDS ON EQUILIBRIUM CASIMIR TORQUE

In this section we consider a Wick rotation consistent with a change of variables $\omega = i\xi$ from ω to ξ. Unless stated otherwise, all quantities in this section are taken to implicitly depend on $i\xi$. Regarding notation, a vector field $\mathbf{v}(\mathbf{x})$ will be denoted by $|\mathbf{v}\rangle$. At $\omega = i\xi$, although all relevant polarization and field quantities as well as $\mathbb{V}$ and $\mathbb{G}_0$ can be defined to be real valued in position space without loss of generality, we still use the Hermitian inner product $\langle\mathbf{u}||\mathbf{v}\rangle = \int d^3x\,\mathbf{u}(\mathbf{x})^*\cdot\mathbf{v}(\mathbf{x})$ since the eigenbasis for which calculations are most convenient can still be complex valued. An operator $\mathbb{A}(\mathbf{x},\mathbf{x}')$ will be denoted by $\mathbb{A}$, with $\int d^3x'\mathbb{A}(\mathbf{x},\mathbf{x}')\cdot\mathbf{v}(\mathbf{x}')$ denoted by $\mathbb{A}|\mathbf{v}\rangle$.

As described in more detail below, following the procedure laid out in Refs. [34–36], and as an exemplary application of Eq. (4), we derive upper and lower bounds on the Casimir torque that may be experienced by a dipolar particle neighboring a structured surface. The torque bounds necessitate only that the design region Ω containing the structured object be rotationally invariant about the same axis going through the dipolar particle about which torque is being considered. The bounds encompass *any* possible structure composed of a homogeneous, local, and isotropic electric susceptibility $\chi(i\xi)$ in the design domain Ω. Concisely, we expand the dipolar response, including local field effects, along its principal axes as $\frac{1}{2}[\mathbb{T}_{\mathrm{dip}}(i\xi) + \mathbb{T}_{\mathrm{dip}}^T(i\xi)] \equiv \sum_a \alpha_a(i\xi)|\mathbf{u}^{(a)}\rangle\langle\mathbf{u}^{(a)}|$, where each $\alpha_a(i\xi) > 0$ is a polarizability component, while $\mathbf{u}^{(a)}(\mathbf{x}) = \mathbf{n}_a\delta^{(3)}(\mathbf{x}-\mathbf{R})$ corresponds to a localized basis function at $\mathbf{R}$ (the dipole location) in the $\mathbf{n}_a$ direction. The chosen design domain Ω enclosing the second object is such that projection into Ω, denoted by $\mathbb{P}(\Omega)$, commutes with the observable of interest $\hat{\Theta}$. Our bounds $\Theta \in [\Theta^-, \Theta^+]$ for $T = 0$ K can be written concisely as

$$\Theta^\pm = \pm\int_0^\infty \frac{d\xi}{2\pi}\sum_a \alpha_a\sqrt{\frac{\langle\mathbf{u}^{(a)},\hat{\Theta}^\dagger\hat{\Theta}\mathbb{G}_{\mathrm{sca}}(\Omega)\mathbf{u}^{(a)}\rangle}{\langle\mathbf{u}^{(a)},\mathbb{G}_{\mathrm{sca}}(\Omega)\mathbf{u}^{(a)}\rangle^{-1}}}, \tag{12}$$

where $\mathbb{G}_{\mathrm{sca}}(\Omega) = \mathbb{G}_0(\chi^{-1}\mathbb{P}(\Omega) - \mathbb{P}(\Omega)\mathbb{G}_0\mathbb{P}(\Omega))^{-1}\mathbb{G}_0$ is the scattering Green's function of the equivalent object formed by filling the entire domain Ω with the susceptibility χ. The maximization and minimization bounds differ in sign, but not magnitude, as expected on physical grounds if $[\hat{\Theta}, \mathbb{P}(\Omega)] = 0$.

A. Derivation

For concreteness, consider the Casimir torque at zero temperature on a dipolar particle, which can be written as

$$\boldsymbol{\tau}_{\rm dip} = \int_0^\infty \frac{d\xi}{2\pi} \mathrm{Re\,Tr}\bigg(\frac{1}{1-\mathbb{G}_0\mathbb{T}_{\rm dip}\mathbb{G}_0\mathbb{T}} \times \mathbb{G}_0(\mathbb{T}_{\rm dip} i\hat{\mathbf{J}} - i\hat{\mathbf{J}}\mathbb{T}_{\rm dip})\mathbb{G}_0\mathbb{T}\bigg), \quad (13)$$

where $\mathbb{T} = (\mathbb{V}^{-1} - \mathbb{G}_0)^{-1} = (1-\mathbb{V}\mathbb{G}_0)^{-1}\mathbb{V}$ and likewise $\mathbb{T}_{\rm dip} = (\mathbb{V}_{\rm dip}^{-1} - \mathbb{G}_0)^{-1} = (1-\mathbb{V}_{\rm dip}\mathbb{G}_0)^{-1}\mathbb{V}_{\rm dip}$. We group i and $\hat{\mathbf{J}}$ together so that all operators are explicitly real valued in position space. To simplify matters, we assume that the dipole is small enough compared to the macroscopic body that multiple scattering effects between different objects can be neglected, though multiple scattering within each object cannot, that is, we replace $(1-\mathbb{T}_{\rm dip}\mathbb{G}_0\mathbb{T}\mathbb{G}_0)^{-1}$ with 1. Also, assume for simplicity that $\mathbb{T}$ is symmetric ($\mathbb{V}$ describes a reciprocal material) but that $\mathbb{T}_{\rm dip}$ can be nonreciprocal. Finally, using the cyclic properties of the trace, the fact that $\hat{J}_k^T = -\hat{J}_k$, and the assumption that $\mathbb{G}_0$ and $\mathbb{T}$ are symmetric yields

$$\tau_{{\rm dip},k} = \int_0^\infty \frac{d\xi}{2\pi} \mathrm{Re\,Tr}\big[\mathbb{G}_0\big(\mathbb{T}_{\rm dip} + \mathbb{T}_{\rm dip}^T\big) i\hat{J}_k \mathbb{G}_0\mathbb{T}\big] \quad (14)$$

$$= \int_0^\infty \frac{d\xi}{2\pi} \mathrm{Re} 2\sum_a \alpha_a \langle \mathbf{u}^{(a)}, i\hat{J}_k\mathbb{G}_0\mathbb{T}\mathbb{G}_0\mathbf{u}^{(a)}\rangle. \quad (15)$$

The torque on the dipole depends only on the symmetric part of $\mathbb{T}_{\rm dip}$, and it is this expression for the torque on the dipole that we will maximize and minimize.

Our derivation of bounds is based on optimization using the principles of Lagrangian duality [45]. The loosest such bound only imposes that the optimal scattering operator satisfies the conservation of power (optical theorem [46]) over the entire design domain and not the full scattering equations. Instead of optimizing over $\mathbb{V}$ which has support in Ω, we relax the problem and instead take as the degree of freedom the induced (polarization) current $|\mathbf{P}^{(a)}\rangle \equiv \mathbb{T}\mathbb{G}_0|\mathbf{u}^{(a)}\rangle$ with support only in the design domain Ω. Since the polarization current is the degree of freedom, the bounds are monotonic with respect to the design domain; any polarization currents explored in an optimization with support within some smaller domain $\Omega' \subset \Omega$ are also explored in the bigger domain Ω. Similar techniques have recently been used to derive bounds on deterministic scattering and nonequilibrium electromagnetic phenomena [13,34–37,47–50]. Concretely, the problem we solve is

$$\max_{\{\mathbf{P}_a(\mathbf{r};i\xi)\in\Omega\}} \int_0^\infty \frac{d\xi}{2\pi} 2\sum_a \alpha_a \mathrm{Re}\langle \mathbf{u}^{(a)}, \mathbb{G}_0 i\hat{J}_k \mathbf{P}^{(a)}\rangle \quad (16a)$$

subject to

$$\mathrm{Re}[\langle \mathbf{u}^{(a)}|\mathbb{G}_0|\mathbf{P}^{(a)}\rangle - \langle \mathbf{P}^{(a)}|\mathbb{P}(\Omega)(\chi^{-1} - \mathbb{G}_0)\mathbb{P}(\Omega)|\mathbf{P}^{(a)}\rangle] = 0 \quad (16b)$$

for all a and each $\xi \geqslant 0$.

First, we consider the problem of maximizing $\mathrm{Re}(2\langle \mathbf{E}^{\rm inc}, i\hat{\Theta}\mathbf{P}\rangle)$. For convenience, we define the eigenvalue decomposition of the projection of $\mathbb{G}_0$ into the domain Ω as $\mathbb{P}(\Omega)\mathbb{G}_0\mathbb{P}(\Omega) = -\sum_\mu g_\mu |\mathbf{N}^{(\mu)}\rangle\langle \mathbf{N}^{(\mu)}|$, where $g_\mu > 0$ and the eigenvectors are orthonormal: $\langle \mathbf{N}^{(\mu)}, \mathbf{N}^{(\nu)}\rangle = \delta_{\mu\nu}$. We also assume that $|\mathbf{N}^{(\mu)}\rangle$ are eigenstates of $\hat{\Theta}$ so that $\hat{\Theta}|\mathbf{N}^{(\mu)}\rangle = \theta_\mu|\mathbf{N}^{(\mu)}\rangle$. For our operators of interest, $\hat{\Theta}^\dagger = \hat{\Theta}$, so the eigenvalues θ_μ are purely real. Since $\hat{\Theta}$ commutes with isotropic $\mathbb{G}_0$, the assumption of simultaneous diagonalization therefore puts restrictions on $\mathbb{P}(\Omega)$, i.e., the geometry of the design domain. We then define the basis expansion coefficients $e_\mu = \langle \mathbf{N}^{(\mu)}, \mathbf{E}^{\rm inc}\rangle$ and $p_\mu = \langle \mathbf{N}^{(\mu)}, \mathbf{P}\rangle$. This leads to a constrained optimization problem with a Lagrangian given by

$$L = \sum_\mu \{\mathrm{Re}(2e_\mu^* p_\mu i\theta_\mu) - \lambda[\mathrm{Re}(e_\mu^* p_\mu) - (\chi^{-1} + g_\mu)p_\mu^* p_\mu]\}, \quad (17)$$

where $\lambda \in \mathbb{R}$ is a Lagrange multiplier.

Carrying out the optimization, we find that $e_\mu^* i\theta_\mu - \lambda[e_\mu^*/2 - (\chi^{-1} + g_\mu)p_\mu^*] = 0$ and $\sum_\mu[\mathrm{Re}(e_\mu^* p_\mu) - (\chi^{-1} + g_\mu)p_\mu^* p_\mu] = 0$. The first equation gives $p_\mu = \frac{e_\mu}{\chi^{-1}+g_\mu}(\frac{1}{2} + \frac{i\theta_\mu}{\lambda})$, which can then be plugged into the second equation to get

$$\lambda = \pm 2\sqrt{\left(\sum_\mu \frac{|e_\mu|^2\theta_\mu^2}{\chi^{-1}+g_\mu}\right)\Bigg/\left(\sum_\mu \frac{|e_\mu|^2}{\chi^{-1}+g_\mu}\right)}$$

$$= \pm 2\sqrt{\frac{\langle \hat{\Theta}\mathbf{E}^{\rm inc}, [\chi^{-1}\mathbb{P}(\Omega) - \mathbb{P}(\Omega)\mathbb{G}_0\mathbb{P}(\Omega)]^{-1}\hat{\Theta}\mathbf{E}^{\rm inc}\rangle}{\langle \mathbf{E}^{\rm inc}, [\chi^{-1}\mathbb{P}(\Omega) - \mathbb{P}(\Omega)\mathbb{G}_0\mathbb{P}(\Omega)]^{-1}\mathbf{E}^{\rm inc}\rangle}}.$$

The objective has $\frac{\delta^2 L}{\delta p_\mu \delta p_\nu^*} = \lambda(\chi^{-1} + g_\mu)\delta_{\mu\nu}$, so the negative value of λ gives the maximum while the positive value gives the minimum. The stationary point corresponding to $\lambda = 0$, which is a saddle point, can occur if $\hat{\Theta}|\mathbf{E}^{\rm inc}\rangle = 0$. However, this cannot occur for the incident field radiated by a dipole into the design domain, so we ignore this mathematical case going forward. Consequently, $L \in [L^-, L^+]$, with

$$L^\pm = \pm\sqrt{\frac{\langle \mathbf{E}^{\rm inc}, \hat{\Theta}^\dagger[\chi^{-1}\mathbb{P}(\Omega) - \mathbb{P}(\Omega)\mathbb{G}_0\mathbb{P}(\Omega)]^{-1}\hat{\Theta}\mathbf{E}^{\rm inc}\rangle}{\langle \mathbf{E}^{\rm inc}, [\chi^{-1}\mathbb{P}(\Omega) - \mathbb{P}(\Omega)\mathbb{G}_0\mathbb{P}(\Omega)]^{-1}\mathbf{E}^{\rm inc}\rangle^{-1}}}. \quad (18)$$

For our problem of interest, Eq. (16a), we set $|\mathbf{E}^{\rm inc}\rangle = \mathbb{G}_0|\mathbf{u}^{(a)}\rangle$ and identify $\mathbb{G}_{\rm sca}(\Omega) = \mathbb{G}_0(\chi^{-1}\mathbb{P}(\Omega) - \mathbb{P}(\Omega)\mathbb{G}_0\mathbb{P}(\Omega))^{-1}\mathbb{G}_0$ as the scattering Green's function of the equivalent object formed by filling the entire domain Ω with the susceptibility χ. Since $\alpha_a(i\xi) > 0$, the net upper bound cannot fall above the upper bound applied to each channel a, just as the net lower bound cannot fall below the per-channel lower bound. This argument also applies to each ξ in the integral. Since it was assumed that $\hat{\Theta}$ and $\mathbb{P}(\Omega)$ commute, one can work with $\mathbb{G}_{\rm sca}(\Omega)$ and $\hat{\Theta}^\dagger\hat{\Theta}\mathbb{G}_{\rm sca}(\Omega)$ instead of evaluating $\hat{\Theta}$ on a vector, yielding Eq. (12).

The extension to $T > 0$ K follows by noting that $\coth(\frac{\hbar\omega}{2k_BT})$ has poles at ω_n satisfying $\frac{\hbar\omega_n}{2k_BT} = i\pi n$ for $n \in \mathbb{Z}$. Thus, closing the contour $\int_{-\infty}^{\infty} d\omega$ into the upper-half plane picks up poles with $\mathrm{Im}(\omega_n) \geqslant 0$, so one only needs to consider $n = 0, 1, \ldots$. The residue of $\coth(\frac{\hbar\omega}{2k_BT})$ at the poles as a function ω is $\frac{2k_BT}{\hbar}$. The indented path around the simple pole at $\omega = 0$ contributes half the residue that a full circle does. Therefore, if the actual observable or its bound at zero

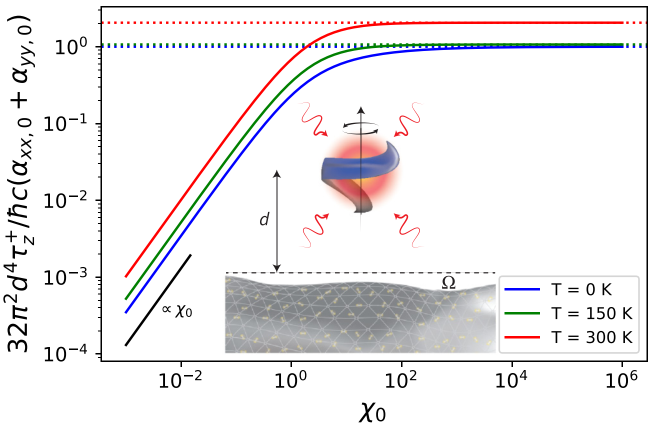

FIG. 1. Material dependence of bounds on Casimir torque. Shown are the upper bounds (solid lines) on the Casimir torque on a nondispersive dipolar particle above a planar half-space design domain Ω which contains a structure made of nondispersive susceptibility χ_0 (inset schematic). The bounds saturate in the perfect electric conductor limit (horizontal dotted lines). At $T=0$ K, the bounds approach $\frac{\hbar c}{32\pi^2 d^4}(\alpha_{xx,0}+\alpha_{yy,0})$ as $\chi_0\to\infty$ and $\frac{7\hbar c}{640\pi^2 d^4}(\alpha_{xx,0}+\alpha_{yy,0})\chi_0$ for $\chi_0 \ll 1$, where d is the distance of the particle to the half-space design domain. The expression for $T>0$ K is more complicated [see Eq. (22)]. The calculations were done with $d = 10$ μm

temperature is written as $F(0)=\int_0^\infty f(i\xi)\frac{d\xi}{2\pi}$ for the corresponding integrand $f(i\xi)$, then the corresponding quantity for temperatures $T>0$ K is $F(T)=\frac{k_B T}{\hbar}\sum_{n=0}^{\prime\infty} f(i\xi_n)$, where the Matsubara frequencies are $\xi_n = 2\pi k_B T n/\hbar$, and the prime on the summation means a prefactor of $\frac{1}{2}$ for the contribution at $n=0$.

B. Numerics, asymptotics, and discussion

For concreteness, we apply this bound expression on the torque about the z axis exerted by structures contained within a planar semi-infinite half space $\Omega=\{(x,y,z)|z\leqslant 0\}$ (Fig. 1 inset), in which case $\mathbb{G}_{\text{sca}}(\Omega)$ and $\hat{J}_z^2\mathbb{G}_{\text{sca}}(\Omega)$ have known semianalytic forms (Appendix B), allowing for evaluation of

$$\tau^{\pm}_{\text{dip},z} = \pm\int_0^\infty \frac{d\xi}{2\pi}\sum_a \alpha_a\sqrt{\frac{\langle \mathbf{u}^{(a)}, \hat{J}_z^2\mathbb{G}_{\text{sca}}(\Omega)\mathbf{u}^{(a)}\rangle}{\langle \mathbf{u}^{(a)}, \mathbb{G}_{\text{sca}}(\Omega)\mathbf{u}^{(a)}\rangle^{-1}}}. \tag{19}$$

This example encompasses a wide variety of possible structure designs, but by no means represents the full extent of the theory; bounds can also be evaluated assuming other design domains such as spherical or cylindrical shells.

For a dipole located at $(0,0,d)$, we find

$$\tau^{\pm}_{\text{dip},z}(T=0) = \pm\frac{\hbar c}{16\pi^2 d^4}\int_0^\infty\int_0^\infty\left[\alpha_{xx}\left(\frac{i\tilde{\xi}c}{d}\right)+\alpha_{yy}\left(\frac{i\tilde{\xi}c}{d}\right)\right]\left(-\frac{\tilde{\xi}^2}{\sqrt{\tilde{\xi}^2+\tilde{k}^2}}\frac{\sqrt{\tilde{\xi}^2+\tilde{k}^2}-\sqrt{[1+\chi(\frac{i\tilde{\xi}c}{d})]\tilde{\xi}^2+\tilde{k}^2}}{\sqrt{\tilde{\xi}^2+\tilde{k}^2}+\sqrt{[1+\chi(\frac{i\tilde{\xi}c}{d})]\tilde{\xi}^2+\tilde{k}^2}}\right.$$
$$\left.+\sqrt{\tilde{\xi}^2+\tilde{k}^2}\frac{[1+\chi(\frac{i\tilde{\xi}c}{d})]\sqrt{\tilde{\xi}^2+\tilde{k}^2}-\sqrt{[1+\chi(\frac{i\tilde{\xi}c}{d})]\tilde{\xi}^2+\tilde{k}^2}}{[1+\chi(\frac{i\tilde{\xi}c}{d})]\sqrt{\tilde{\xi}^2+\tilde{k}^2}+\sqrt{[1+\chi(\frac{i\tilde{\xi}c}{d})]\tilde{\xi}^2+\tilde{k}^2}}\right)e^{-2\sqrt{\tilde{\xi}^2+\tilde{k}^2}}\tilde{k}\,d\tilde{k}\,d\tilde{\xi}, \tag{20}$$

$$\tau^{\pm}_{\text{dip},z}(T>0) = \pm\frac{k_B T}{8\pi d^3}\sum_{n=0}^{\infty}{}'[\alpha_{xx}(i\xi_n)+\alpha_{yy}(i\xi_n)]\int_0^\infty\left(-\frac{(\xi_n d/c)^2}{\sqrt{(\xi_n d/c)^2+\tilde{k}^2}}\frac{\sqrt{(\xi_n d/c)^2+\tilde{k}^2}-\sqrt{[1+\chi(i\xi_n)](\xi_n d/c)^2+\tilde{k}^2}}{\sqrt{(\xi_n d/c)^2+\tilde{k}^2}+\sqrt{[1+\chi(i\xi_n)](\xi_n d/c)^2+\tilde{k}^2}}\right.$$
$$\left.+\sqrt{(\xi_n d/c)^2+\tilde{k}^2}\frac{[1+\chi(i\xi_n)]\sqrt{(\xi_n d/c)^2+\tilde{k}^2}-\sqrt{[1+\chi(i\xi_n)](\xi_n d/c)^2+\tilde{k}^2}}{[1+\chi(i\xi_n)]\sqrt{(\xi_n d/c)^2+\tilde{k}^2}+\sqrt{[1+\chi(i\xi_n)](\xi_n d/c)^2+\tilde{k}^2}}\right)e^{-2\sqrt{(\xi_n d/c)^2+\tilde{k}^2}}\tilde{k}\,d\tilde{k}. \tag{21}$$

Assume for simplicity that the polarizabilities are also dispersionless. In such a case, the bounds on the torque can be written as $\tau^{\pm}_{\text{dip},z}(T=0)=\pm(\alpha_{xx,0}+\alpha_{yy,0})\frac{\hbar c}{16\pi^2 d^4}g[\chi(i\tilde{\xi}c/d)]$ for some dimensionless functional g which depends only on the macroscopic susceptibility χ evaluated at a frequency dependent on the separation d. We first consider a macroscopic body of dispersionless susceptibility $\chi(i\xi)=\chi_0$. See Fig. 1 for a numerical evaluation of the bounds. The bounds scale linearly [$\frac{7\hbar c}{640\pi^2 d^4}(\alpha_{xx,0}+\alpha_{yy,0})\chi_0$ for $T=0$ K] as a function of χ_0 for $\chi_0\ll 1$ and goes to 0 as $\chi_0\to 0$, as expected since $\chi_0 = 0$ implies the design domain is only vacuum, in which case the equilibrium torque on the isolated dipole is identically 0. The bounds increase monotonically with χ_0. Monotonicity can also be expected from Eq. (19) since, expanding $|\mathbf{E}^{(a)}_{\text{inc}}\rangle \equiv \mathbb{G}_0|\mathbf{u}^{(a)}\rangle$ in the basis defined in the previous section, $\sqrt{\langle \mathbf{u}^{(a)}, \hat{\Theta}^\dagger\mathbb{G}_{\text{sca}}(\Omega)\hat{\Theta}\mathbf{u}^{(a)}\rangle\langle \mathbf{u}^{(a)}, \mathbb{G}_{\text{sca}}(\Omega)\mathbf{u}^{(a)}\rangle}$ expands to $\sqrt{(\sum_\mu \frac{|e^{(a)}_\mu|^2|\theta_\mu|^2}{\chi^{-1}+g_\mu})(\sum_\mu \frac{|e^{(a)}_\mu|^2}{\chi^{-1}+g_\mu})}$, from which it is clear that an increase in $\chi(i\xi)$ can only increase the contribution to the bound at a given ξ. This holds for any ξ and, since $\alpha_a>0$, therefore for the total integrated ($T=0$ K) or summed ($T>0$ K) quantities as well. However, the bounds do not diverge but rather saturate to a finite value in the perfect electrical conductor (PEC) limit $\chi_0\to\infty$. In the PEC limit, the integrals and summations can be done explicitly and we find

$$\tau^{\text{PEC},\pm}_{\text{dip}} = \begin{cases}\pm\frac{\hbar c}{32\pi^2 d^4}(\alpha_{xx,0}+\alpha_{yy,0}), & T=0\\ \pm\frac{\hbar c}{32\pi^2 d^4}(\alpha_{xx,0}+\alpha_{yy,0})\frac{a}{2}\frac{1+(8a^2-4a-1)e^{2a}+(8a^2+4a-1)e^{4a}+e^{6a}}{2(e^{2a}-1)^3}, & T>0,\end{cases} \tag{22}$$

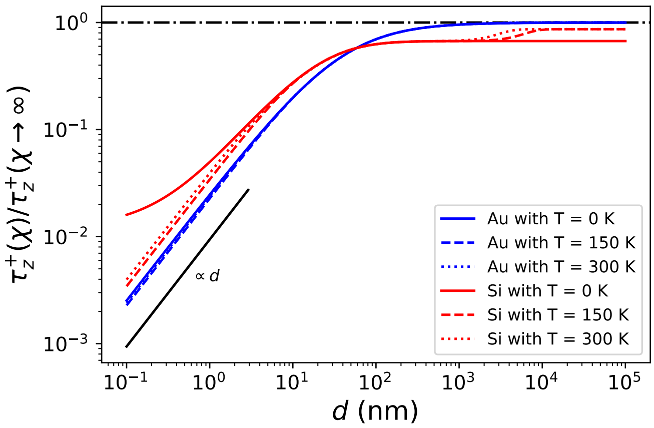

FIG. 2. Distance dependence of bounds on Casimir torque for gold and silicon structures. Shown are upper bounds to the Casimir torque on a nondispersive dipole above a planar half-space design domain which contains a structure with a macroscopic susceptibility χ corresponding to that of gold or silicon. The results are normalized by the perfect electrical conductor limit given by Eq. (22).

where $a \equiv \frac{2\pi k_B T d}{\hbar c}$. For $T \ll \frac{\hbar c}{2\pi k_B d}$ we find

$$\frac{\tau^{\pm}_{\mathrm{dip}}(\chi_0\to\infty, T>0)}{\tau^{\pm}_{\mathrm{dip}}(\chi_0\to\infty, T=0)} = \left[1-\frac{1}{45}\left(\frac{2\pi k_B T d}{\hbar c}\right)^4 + O(T^6)\right], \tag{23}$$

while for $T \gg \frac{\hbar c}{2\pi k_B d}$,

$$\frac{\tau^{\pm}_{\mathrm{dip}}(\chi_0\to\infty, T>0)}{\tau^{\pm}_{\mathrm{dip}}(\chi_0\to\infty, T=0)} = \left(\frac{1}{4}\frac{2\pi k_B T d}{\hbar c} + O(T^2)\right), \tag{24}$$

so nonzero temperature T changes the exact d^{-4} distance scaling of the bounds. Although the bounds are applicable at any temperature and any appropriate local, homogeneous, isotropic model of material dispersion, the PEC limit, despite resulting in a looser bound, has the benefit of being analytic, resulting in easier extraction of scaling behavior.

Next we relax the assumption that $\chi(i\xi)$ is nondispersive and consider the particular cases of (i) a gold medium with electric susceptibility modeled by $\chi_{\mathrm{Au}}(i\xi) = \omega_p^2/(\xi^2+\gamma\xi)$, where $\omega_p = 1.37\times10^{16}$ rad/s and $\gamma = 5.32\times10^{13}$ rad/s, and (ii) intrinsic (undoped) silicon with $\chi_{\mathrm{Si}}(i\xi) = \epsilon_{\mathrm{Si}}(\infty) - 1 + [\epsilon_{\mathrm{Si}}(0)+\epsilon_{\mathrm{Si}}(\infty)]/(1+\xi^2/\omega_0^2)$, where $\epsilon_{\mathrm{Si}}(0) = 11.87$, $\epsilon_{\mathrm{Si}}(\infty) = 1.035$, and $\omega_0 = 6.6\times10^{15}$ rad/s [36]. For simplicity, we continue to neglect dispersion in α_{xx} and α_{yy}. See Fig. 2. For $d > 1\ \mu$m, we find that $\tau^{\pm}_{\mathrm{dip},z}(\chi_{\mathrm{Au}})$ is within 5% of the PEC limit and within 1% for $d > 10\ \mu$m, regardless of the temperature.

IV. CONCLUSION

In summary, we presented trace expressions for equilibrium Casimir torque that apply to arbitrary object shapes and materials, generalizing prior work on power transfer [33,43,51] and forces [36,38,43]. The need for a full account of the spin and orbital angular momentum carried by waves in this setting is explicit in the trace expressions. Then, using the derived trace expressions, we calculated bounds on the Casimir torque on a dipolar particle next to a structure of isotropic susceptibility χ enclosed within a prescribed domain and evaluated the bounds specifically for a half-space design domain as a demonstrative example. An interesting direction for future work is the extension of the bounds for the case where the structured medium is birefringent or, more generally, anisotropic.

ACKNOWLEDGMENTS

B.S. thanks Prashanth S. Venkataram and Pengning Chao for helpful discussions. This work was supported by the National Science Foundation under the Emerging Frontiers in Research and Innovation Program No. EFMA-1640986, the Cornell Center for Materials Research through Award No. DMR-1719875, the Defense Advanced Research Projects Agency under Agreements No. HR00112090011, No. HR00111820046, and No. HR0011047197. The views, opinions, and findings expressed herein are those of the authors and should not be interpreted as representing the official views or policies of any institution.

APPENDIX A: TRACE EXPRESSIONS FOR NONRECIPROCAL MATERIALS

In this Appendix we provide the intermediate steps in the derivation of the trace expressions for the torque in terms of the scattering operators and the background Green's function.

1. Single object

For the case of a single object (reciprocal or nonreciprocal), we use $\mathbb{G} = \mathbb{G}_0 + \mathbb{G}_0\mathbb{T}\mathbb{G}_0$ to find that

$$\mathrm{Tr}|_V\left(\hat{\mathbf{J}}\mathbb{G}^{\mathsf{A}}\mathbb{G}_0^{-1\dagger}\right) = \mathrm{Tr}|_V[\hat{\mathbf{J}}(\mathbb{G}_0\mathbb{T} - \mathbb{G}_0^{\dagger}\mathbb{T}^{\dagger})]\frac{1}{2i} \tag{A1}$$

$$= \mathrm{Tr}[\hat{\mathbf{J}}(\mathbb{G}_0\mathbb{T} - \mathbb{G}_0^{\dagger}\mathbb{T}^{\dagger})]\frac{1}{2i}, \tag{A2}$$

where the first equality follows since $\frac{\omega^2}{c^2}\mathbb{G}_0^{-1} = \nabla\times\nabla\times -\frac{\omega^2}{c^2}$ inside the body and so gives the identity operator when acting on $\mathbb{G}_0$ or $\mathbb{G}_0^{\dagger}$ which has one argument restricted to the body. In more detail, $\mathbb{G}_0^{-1\dagger} = \mathbb{G}_0^{-1} - 2i\mathbb{G}_0^{-1\mathsf{A}}$, where $\mathbb{G}_0^{-1\mathsf{A}}$ is local and infinitesimal (it is proportional to $\mathbb{V}^{\mathsf{A}}_{\mathrm{env}}$). The $\mathbb{V}^{\mathsf{A}}_{\mathrm{env}}$ term is the famous environmental "dust" contribution [38,52]. Its contribution is infinitesimal if integrated over a finite region, but it can be noninfinitesimal if integrated over infinite space. The second equality follows since the $\mathbb{T}$ operator vanishes unless both arguments are inside the body, so the integration can be extended to the entire space. Therefore,

$$\boldsymbol{\tau}^{(\mathrm{eq})} = -\mathrm{Im}\int_{-\infty}^{\infty}\frac{d\omega}{2\pi}\coth\left(\frac{\hbar\omega}{2k_BT}\right)\mathrm{Tr}|_V\left(\hat{\Theta}\mathbb{G}^{\mathsf{A}}\mathbb{G}_0^{-1\dagger}\right) \tag{A3}$$

$$= \mathrm{Re}\int_{-\infty}^{\infty}\frac{d\omega}{4\pi}\coth\left(\frac{\hbar\omega}{2k_BT}\right)\mathrm{Tr}[\hat{\mathbf{J}}(\mathbb{G}_0\mathbb{T} - \mathbb{G}_0^{\dagger}\mathbb{T}^{\dagger})]. \tag{A4}$$

Using $\mathrm{Re}\,\mathrm{Tr}(A) = \mathrm{Re}\,\mathrm{Tr}(A^{\dagger})$, $\hat{\mathbf{J}} = \hat{\mathbf{J}}^{\dagger}$, $\hat{\mathbf{J}}\mathbb{G}_0 = \mathbb{G}_0\hat{\mathbf{J}}$, and the cyclicity of the trace, one finds that $\mathrm{Re}\,\mathrm{Tr}[\hat{\mathbf{J}}(\mathbb{G}_0\mathbb{T} - \mathbb{G}_0^{\dagger}\mathbb{T}^{\dagger})] = 0$ for any $\mathbb{T}$.

2. Two or more objects

We start with

$$\mathbb{G} = (1+\mathbb{G}_0\mathbb{T}_{\bar{1}})\frac{1}{1-\mathbb{G}_0\mathbb{T}_1\mathbb{G}_0\mathbb{T}_{\bar{1}}}(1+\mathbb{G}_0\mathbb{T}_1)\mathbb{G}_0 \tag{A5}$$

$$= (1+\mathbb{G}_0\mathbb{T}_1)\frac{1}{1-\mathbb{G}_0\mathbb{T}_{\bar{1}}\mathbb{G}_0\mathbb{T}_1}(1+\mathbb{G}_0\mathbb{T}_{\bar{1}})\mathbb{G}_0. \tag{A6}$$

The relevant expression for $\mathbb{G}$ is the one for which the rightmost $\mathbb{T}$ operator is nonzero in the volume being integrated over. This is because $\mathbb{T}_\alpha$ vanishes outside the volume of α, allowing for the extension of the volume integration to be over all space, which results in a basis-independent trace expression. Collecting terms with $\mathbb{T}_1$ as the rightmost term, we find

$$\boldsymbol{\tau}^{(1,\mathrm{eq})} = -\mathrm{Im}\int_{-\infty}^{\infty}\frac{d\omega}{2\pi}\coth\left(\frac{\hbar\omega}{2k_BT}\right)\mathrm{Tr}|_{V_1}\big(\hat{\mathbf{J}}\mathbb{G}^{\mathsf{A}}\mathbb{G}_0^{-1\dagger}\big) \tag{A7}$$

$$= -\mathrm{Im}\int_{-\infty}^{\infty}\frac{d\omega}{2\pi}\coth\left(\frac{\hbar\omega}{2k_BT}\right)\Bigg[\mathrm{Tr}\Bigg(\hat{\mathbf{J}}(1+\mathbb{G}_0\mathbb{T}_{\bar{1}})\frac{1}{1-\mathbb{G}_0\mathbb{T}_1\mathbb{G}_0\mathbb{T}_{\bar{1}}}\mathbb{G}_0\mathbb{T}_1\Bigg) - \mathrm{Tr}\Bigg(\hat{\mathbf{J}}\mathbb{G}_0^\dagger(1+\mathbb{T}_{\bar{1}}^\dagger\mathbb{G}_0^\dagger)\frac{1}{1-\mathbb{T}_1^\dagger\mathbb{G}_0^\dagger\mathbb{T}_{\bar{1}}^\dagger\mathbb{G}_0^\dagger}\mathbb{T}_1^\dagger\Bigg)\Bigg]\frac{1}{2i} \tag{A8}$$

$$= \mathrm{Re}\int_{-\infty}^{\infty}\frac{d\omega}{4\pi}\coth\left(\frac{\hbar\omega}{2k_BT}\right)\Bigg[\mathrm{Tr}\Bigg(\hat{\mathbf{J}}(1+\mathbb{G}_0\mathbb{T}_{\bar{1}})\frac{1}{1-\mathbb{G}_0\mathbb{T}_1\mathbb{G}_0\mathbb{T}_{\bar{1}}}\mathbb{G}_0\mathbb{T}_1\Bigg) - \mathrm{Tr}\Bigg(\hat{\mathbf{J}}\mathbb{G}_0^\dagger(1+\mathbb{T}_{\bar{1}}^\dagger\mathbb{G}_0^\dagger)\frac{1}{1-\mathbb{T}_1^\dagger\mathbb{G}_0^\dagger\mathbb{T}_{\bar{1}}^\dagger\mathbb{G}_0^\dagger}\mathbb{T}_1^\dagger\Bigg)\Bigg]. \tag{A9}$$

Applying $\mathrm{Re}\,\mathrm{Tr}(A) = \mathrm{Re}\,\mathrm{Tr}(A^\dagger)$ to the second trace term leads to

$$\boldsymbol{\tau}^{(1,\mathrm{eq})} = \mathrm{Re}\int_{-\infty}^{\infty}\frac{d\omega}{4\pi}\coth\left(\frac{\hbar\omega}{2k_BT}\right)\mathrm{Tr}\Bigg((\hat{\mathbf{J}}\mathbb{G}_0\mathbb{T}_{\bar{1}} - \mathbb{G}_0\mathbb{T}_{\bar{1}}\hat{\mathbf{J}})\frac{1}{1-\mathbb{G}_0\mathbb{T}_1\mathbb{G}_0\mathbb{T}_2}\mathbb{G}_0\mathbb{T}_1\Bigg) \tag{A10}$$

$$= \mathrm{Re}\int_0^{\infty}\frac{d\omega}{\pi}\left[n(\omega,T)+\frac{1}{2}\right]\mathrm{Tr}\Bigg(\frac{1}{1-\mathbb{G}_0\mathbb{T}_1\mathbb{G}_0\mathbb{T}_{\bar{1}}}\mathbb{G}_0(\mathbb{T}_1\hat{\mathbf{J}} - \hat{\mathbf{J}}\mathbb{T}_1)\mathbb{G}_0\mathbb{T}_{\bar{1}}\Bigg), \tag{A11}$$

which is precisely Eq. (4) when $\alpha = 1$. It is clear that the derivation for $\bar{1}$ is analogous but with $1 \leftrightarrow \bar{1}$ in intermediate expressions,

$$\boldsymbol{\tau}^{(\bar{1},\mathrm{eq})} = -\mathrm{Im}\int_{-\infty}^{\infty}\frac{d\omega}{2\pi}\coth\left(\frac{\hbar\omega}{2k_BT}\right)\mathrm{Tr}|_{V_{\bar{1}}}\big(\hat{\mathbf{J}}\mathbb{G}^{\mathsf{A}}\mathbb{G}_0^{-1\dagger}\big) \tag{A12}$$

$$= \mathrm{Re}\int_0^{\infty}\frac{d\omega}{\pi}\left[n(\omega,T)+\frac{1}{2}\right]\mathrm{Tr}\Bigg(\frac{1}{1-\mathbb{G}_0\mathbb{T}_{\bar{1}}\mathbb{G}_0\mathbb{T}_1}\mathbb{G}_0(\mathbb{T}_{\bar{1}}\hat{\mathbf{J}} - \hat{\mathbf{J}}\mathbb{T}_{\bar{1}})\mathbb{G}_0\mathbb{T}_1\Bigg), \tag{A13}$$

which proves Eq. (4) for $\alpha = \bar{1}$. Note that the above equations are valid for reciprocal and nonreciprocal objects since the intermediate steps in the derivation did not assume reciprocity of the $\mathbb{T}$ operators.

APPENDIX B: GREEN'S-FUNCTION EXPRESSIONS IN REAL SPACE

Here we provide the expressions for the Green's function necessary to compute bounds above a half-space design region.

Here $\mathbb{G}_0$ is defined as the operator that is the inverse of the Maxwell operator, satisfying $[(\nabla\times\nabla\times) - (\omega/c)^2\mathbb{I}]\mathbb{G}_0(\omega,\mathbf{x},\mathbf{x}') = (\omega/c)^2\mathbb{I}\delta^{(3)}(\mathbf{x}-\mathbf{x}')$. In position space and evaluating at $\omega = i\xi$, this yields the expression $\mathbb{G}_0(i\xi,\mathbf{x},\mathbf{x}') = [\nabla\otimes\nabla - (\xi/c)^2](e^{-\xi|\mathbf{x}-\mathbf{x}'|/c}/4\pi|\mathbf{x}-\mathbf{x}'|)$.

The scattering Green's function at $\omega = i\xi$ in the vacuum region above a uniform planar semi-infinite half space of susceptibility χ is [44]

$$\mathbb{G}_{\mathrm{sca}}(i\xi,\mathbf{x},\mathbf{x}') = \frac{1}{2}\int_{-\infty}^{\infty}\int_{-\infty}^{\infty}[\mathbb{M}^{\mathrm{s}}(i\xi,\mathbf{k}) + \mathbb{M}^{\mathrm{p}}(i\xi,\mathbf{k})]e^{i[k_x(x-x')+k_y(y-y')]-\kappa_z(z+z')}\frac{dk_xdk_y}{(2\pi)^2}, \tag{B1}$$

defined in terms of the Cartesian tensors

$$\mathbb{M}^{\mathrm{s}}(i\xi,\mathbf{k}) = -\frac{\xi^2 r^{\mathrm{s}}(i\xi,k)}{c^2\kappa_z k^2}\begin{bmatrix} k_y^2 & -k_xk_y & 0 \\ -k_xk_y & k_x^2 & 0 \\ 0 & 0 & 0 \end{bmatrix}, \tag{B2}$$

$$\mathbb{M}^{\mathrm{p}}(i\xi,\mathbf{k})=\frac{r^{\mathrm{p}}(i\xi,k)}{k^2}\begin{bmatrix}\kappa_z k_x^2 & \kappa_z k_x k_y & -ik^2k_x\\ \kappa_z k_x k_y & \kappa_z k_y^2 & -ik^2 k_y\\ ik^2k_x & ik^2k_y & k^4/\kappa_z\end{bmatrix}, \tag{B3}$$

which are in turn defined in terms of $\mathbf{k}=k_x\mathbf{e}_x+k_y\mathbf{e}_y$, $k=|\mathbf{k}|$, $\kappa_z=\sqrt{(\xi/c)^2+k^2}$, and the Fresnel reflection coefficients

$$r^{\mathrm{s}}(i\xi,k)=\frac{\sqrt{(\xi/c)^2+k^2}-\sqrt{(1+\chi)(\xi/c)^2+k^2}}{\sqrt{(\xi/c)^2+k^2}+\sqrt{(1+\chi)(\xi/c)^2+k^2}}, \tag{B4}$$

$$r^{\mathrm{p}}(i\xi,k)=\frac{(1+\chi)\sqrt{(\xi/c)^2+k^2}-\sqrt{(1+\chi)(\xi/c)^2+k^2}}{(1+\chi)\sqrt{(\xi/c)^2+k^2}+\sqrt{(1+\chi)(\xi/c)^2+k^2}} \tag{B5}$$

at $\omega=i\xi$. To evaluate $\mathbb{G}_{\mathrm{sca}}(i\xi,\mathbf{x},\mathbf{x}')$ in torque settings, polar coordinates are a more natural choice, that is, we reparametrize (k_x,k_y) as (k,ψ) and (x,y,z) as (ρ,ϕ,z) so that

$$\mathbb{G}_{\mathrm{sca}}(i\xi,\mathbf{x},\mathbf{x}')=\frac{1}{2}\int_0^{2\pi}\int_0^{\infty}[\mathbb{M}^{\mathrm{s}}(i\xi,\mathbf{k})+\mathbb{M}^{\mathrm{p}}(i\xi,\mathbf{k})]e^{i\{k\cos(\psi)[\rho\cos(\phi)-\rho'\cos(\phi')]+k\sin(\psi)[\rho\sin(\phi)-\rho'\sin(\phi')]\}-\kappa_z(z+z')}\frac{k\,dk\,d\psi}{(2\pi)^2}. \tag{B6}$$

We then find (defining $\hat{R}_z\equiv\frac{1}{\hbar}\hat{S}_z$)

$$(\hat{J}_z\mathbb{G}_{\mathrm{sca}})(i\xi,\mathbf{x},\mathbf{x}')=\frac{\hbar}{2}\int_0^{2\pi}\int_0^{\infty}[-k\cos(\psi)\rho\sin(\phi)+k\sin(\psi)\rho\cos(\phi)+\hat{R}_z][\mathbb{M}^{\mathrm{s}}(i\xi,\mathbf{k})+\mathbb{M}^{\mathrm{p}}(i\xi,\mathbf{k})]$$
$$\times\, e^{i\{k\cos(\psi)[\rho\cos(\phi)-\rho'\cos(\phi')]+k\sin(\psi)[\rho\sin(\phi)-\rho'\sin(\phi')]\}-\kappa_z(z+z')}\frac{k\,dk\,d\psi}{(2\pi)^2} \tag{B7}$$

and

$$(\hat{J}_z^2\mathbb{G}_{\mathrm{sca}})(i\xi,\mathbf{x},\mathbf{x}')=\frac{\hbar^2}{2}\int_0^{2\pi}\int_0^{\infty}\big\{[-k\cos(\psi)\rho\sin(\phi)+k\sin(\psi)\rho\cos(\phi)]^2-i[-k\cos(\psi)\rho\cos(\phi)-k\sin(\psi)\rho\sin(\phi)]$$
$$+2\hat{R}_z[-k\cos(\psi)\rho\sin(\phi)+k\sin(\psi)\rho\cos(\phi)]+\hat{R}_z^2\big\}[\mathbb{M}^{\mathrm{s}}(i\xi,\mathbf{k})+\mathbb{M}^{\mathrm{p}}(i\xi,\mathbf{k})]$$
$$\times\, e^{i\{k\cos(\psi)[\rho\cos(\phi)-\rho'\cos(\phi')]+k\sin(\psi)[\rho\sin(\phi)-\rho'\sin(\phi')]\}-\kappa_z(z+z')}\frac{k\,dk\,d\psi}{(2\pi)^2}. \tag{B8}$$

We are interested in the torque about the center of mass of the dipole. For $\mathbf{x}=\mathbf{x}'=(0,0,d)$ we get

$$\big(\hat{J}_z^2\mathbb{G}_{\mathrm{sca}}\big)(i\xi,d\mathbf{e}_z,d\mathbf{e}_z)=\frac{\hbar^2}{2}\int_0^{2\pi}\int_0^{\infty}\hat{R}_z^2[\mathbb{M}^{\mathrm{s}}(i\xi,\mathbf{k})+\mathbb{M}^{\mathrm{p}}(i\xi,\mathbf{k})]e^{-2\kappa_z d}\frac{k\,dk\,d\psi}{(2\pi)^2} \tag{B9}$$

$$=\frac{\hbar^2}{2}\int_0^{2\pi}\int_0^{\infty}\begin{bmatrix}1&0&0\\0&1&0\\0&0&0\end{bmatrix}[\mathbb{M}^{\mathrm{s}}(i\xi,\mathbf{k})+\mathbb{M}^{\mathrm{p}}(i\xi,\mathbf{k})]e^{-2\kappa_z d}\frac{k\,dk\,d\psi}{(2\pi)^2}. \tag{B10}$$

It makes intuitive sense that $(\hat{J}_z\mathbb{G}_{\mathrm{sca}})(i\xi,d\mathbf{e}_z,d\mathbf{e}_z)=(\hat{S}_z\mathbb{G}_{\mathrm{sca}})(i\xi,d\mathbf{e}_z,d\mathbf{e}_z)$ since a point dipole has no geometric structure so any torque on it must come from the internal structure (the polarizability matrix). These expressions, after changing to dimensionless integration variables, lead to Eq. (20) in the main text. Explicitly, in the limit that $\chi\to\infty$, then $r^{\mathrm{s}}\to -1$ and $r^{\mathrm{p}}\to 1$, leading to the simplification

$$(\mathbb{G}_{\mathrm{sca}})(i\xi,d\mathbf{e}_z,d\mathbf{e}_z)=\frac{1}{2}\int_0^{2\pi}\int_0^{\infty}\left(\frac{\xi^2}{c^2\kappa_z k^2}\begin{bmatrix}k^2\sin(\psi)^2 & -k^2\cos(\psi)\sin(\psi) & 0\\ -k^2\cos(\psi)\sin(\psi) & k^2\cos(\psi)^2 & 0\\ 0&0&0\end{bmatrix}\right.$$
$$\left.+\frac{1}{k^2}\begin{bmatrix}\kappa_z k^2\cos(\psi)^2 & \kappa_z k^2\cos(\psi)\sin(\psi) & -ik^3\cos(\psi)\\ \kappa_z k^2\cos(\psi)\sin(\psi) & \kappa_z k^2\sin(\psi)^2 & -ik^3\sin(\psi)\\ ik^3\cos(\psi) & ik^3\sin(\psi) & k^4/\kappa_z\end{bmatrix}\right)e^{-2\kappa_z d}\frac{k\,dk\,d\psi}{(2\pi)^2} \tag{B11}$$

$$=\frac{1}{32\pi d^3}\left[1+2\left(\frac{\xi d}{c}\right)+4\left(\frac{\xi d}{c}\right)^2\right]\exp\left(-2\frac{\xi d}{c}\right)\begin{bmatrix}1&0&0\\0&1&0\\0&0&0\end{bmatrix}$$
$$+\frac{1}{16\pi d^3}\left[1+2\left(\frac{\xi d}{c}\right)\right]\exp\left(-2\frac{\xi d}{c}\right)\begin{bmatrix}0&0&0\\0&0&0\\0&0&1\end{bmatrix}. \tag{B12}$$

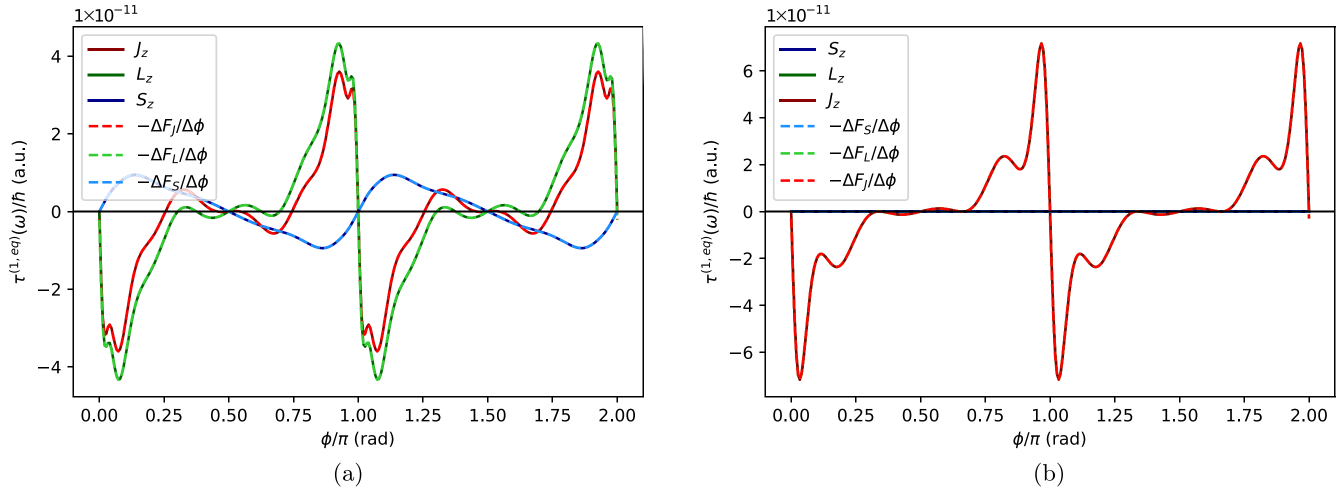

FIG. 3. Torque on the top wire as a function of angle ϕ between the two wires separated by a fixed distance: (a) two birefringent wires and (b) InSb thin wires in the xy plane subject to an external 1.0-T magnetic field in the z direction. Here $T = 300$ K, $\omega = k_B T/\hbar = 3.92 \times 10^{13}$, the length of each wire is $L = 4\pi c/\omega = 96.087$ µm, and the separation is $d = L/10 = 9.6087$ µm.

In the $\chi \to \infty$ limit, $\hat{J}_z^2 \mathbb{G}_{\rm sca}(i\xi, d\mathbf{e}_z, d\mathbf{e}_z)$ is the same as the upper left 2×2 block as above but with an additional factor of $\hbar^2$. These expressions lead directly to Eq. (22) after doing the remaining integration over ξ.

APPENDIX C: TORQUE EXPRESSION IN THE POINT-PARTICLE LIMIT IN THE TWO-BODY CASE

Using the point particle limit and the Born approximation, a simplified expression for the torque exerted on particle 1 is (assuming reciprocity of the materials)

$$\boldsymbol{\tau}^{(1,\rm eq)}(T) = \mathrm{Re}\frac{2}{\pi}\int_0^\infty d\omega\Big[n(\omega,T)+\frac{1}{2}\Big]\mathrm{Tr}(\hat{\mathbf{J}}\mathbb{G}_0\mathbb{T}_2\mathbb{G}_0\mathbb{T}_1). \tag{C1}$$

Using the scattering operators in the small-sphere limit [53],

$$\mathrm{Tr}(\hat{J}_z\mathbb{G}_0\mathbb{T}_2\mathbb{G}_0\mathbb{T}_1) = \mathrm{Re}\,9\int_{V_1} d^3\mathbf{r}\int_{V_2} d^3\mathbf{r}'(\hat{J}_z\mathbb{G}_0)_{ab}(\mathbf{r},\mathbf{r}') \times \left(\frac{\overline{\overline{\epsilon}}_2-1}{\overline{\overline{\epsilon}}_2+2}\right)_{bc}\mathbb{G}_{0,cd}(\mathbf{r}',\mathbf{r})\left(\frac{\overline{\overline{\epsilon}}_1-1}{\overline{\overline{\epsilon}}_1+2}\right)_{da}. \tag{C2}$$

Since the dimensions of the point particles are assumed small compared to any other dimensions in the problem, $(\hat{J}_z\mathbb{G}_0)(\mathbf{r},\mathbf{r}')$ and $\mathbb{G}_0(\mathbf{r}',\mathbf{r})$ do not vary significantly between different points in the different particles. Letting $\mathbf{r}_1$ and $\mathbf{r}_2$ denote the centers of particle 1 and particle 2, respectively, the integrals $\int_{V_1}$ and $\int_{V_2}$ simply introduce factors of $4\pi R_1^3/3$ and $4\pi R_2^3/3$ so that the torque is proportional to the volumes of the spherical particles. Compactly,

$$\boldsymbol{\tau}^{(1,\rm eq)}(T) = \mathrm{Re}\frac{2}{\pi}\int_0^\infty d\omega\Big[n(\omega,T)+\frac{1}{2}\Big]\mathrm{Tr}_{cmp} \times [\hat{\mathbf{J}}\mathbb{G}_0(\mathbf{r}_1,\mathbf{r}_2)\overline{\overline{\alpha}}_2\mathbb{G}_0(\mathbf{r}_2,\mathbf{r}_1)\overline{\overline{\alpha}}_1], \tag{C3}$$

where Tr_{cmp} means a trace only over the vector components ($\mathrm{Tr}_{cmp}[\mathbb{A}(\mathbf{r},\mathbf{r}')] \equiv \sum_a \mathbb{A}_{aa}(\mathbf{r},\mathbf{r}')$) and we introduce polarizability tensors $\overline{\overline{\alpha}}_1$ and $\overline{\overline{\alpha}}_2(\omega) \equiv 4\pi R_2^3\frac{\overline{\overline{\epsilon}}_2(\omega)-\mathbb{I}}{\overline{\overline{\epsilon}}_2(\omega)+2\mathbb{I}}$ located a positions $\mathbf{r}_1$ and $\mathbf{r}_2$, respectively. For the general nonreciprocal case, similar arguments lead to

$$\boldsymbol{\tau}^{(1,\rm eq)}(T) = \mathrm{Re}\frac{1}{\pi}\int_0^\infty d\omega\Big[n(\omega,T)+\frac{1}{2}\Big]\mathrm{Tr} \times [\mathbb{G}_0(\mathbb{T}_1\hat{\mathbf{J}}-\hat{\mathbf{J}}\mathbb{T}_1)\mathbb{G}_0\mathbb{T}_2] \tag{C4}$$

$$= \mathrm{Re}\frac{1}{\pi}\int_0^\infty d\omega\Big[n(\omega,T)+\frac{1}{2}\Big]\mathrm{Tr}_{cmp} \times [\hat{\mathbf{J}}\mathbb{G}_0(\mathbf{r}_1,\mathbf{r}_2)\overline{\overline{\alpha}}_2\mathbb{G}_0(\mathbf{r}_2,\mathbf{r}_1)\overline{\overline{\alpha}}_1 - \hat{\mathbf{J}}\mathbb{G}_0(\mathbf{r}_2,\mathbf{r}_1)\overline{\overline{\alpha}}_1\mathbb{G}_0(\mathbf{r}_1,\mathbf{r}_2)\overline{\overline{\alpha}}_2]. \tag{C5}$$

APPENDIX D: NUMERICAL EXAMPLES IN THE DILUTE LIMIT

A natural question is how the magnitude of contributions of the orbital and spin terms in the torque expression compare. The comparison of the contributions of the orbital and spin terms simplifies greatly in the dilute limit, for which one can approximate each $\mathbb{T}$ operator as $\mathbb{T} = \mathbb{V}(1-\mathbb{G}_0\mathbb{V})^{-1} \approx \mathbb{V}$. In such limits, one can easily create scenarios for which (a) $\tau_{L_z} \neq 0$ and $\tau_{S_z} \neq 0$, (b) $\tau_{L_z} \neq 0$ but $\tau_{S_z} = 0$, and (c) $\tau_{L_z} = 0$ but $\tau_{S_z} \neq 0$.

Consider two thin wires parallel to the x-y plane, separated by a distance d in the z direction with an angle of orientation ϕ between the wires ($\phi = 0$ corresponding to parallel wires). To simplify the numerics, we focus on a single angular frequency ω. In such a case, one can approximate each $\mathbb{T}$ operator as

$$\mathbb{T}(\mathbf{r},\mathbf{r}') = \begin{cases}(\overline{\overline{\epsilon}}-\mathbb{I})\delta(\mathbf{r},\mathbf{r}') & \text{for } \mathbf{r},\mathbf{r}' \in V_{\rm wire}\\ 0 & \text{otherwise,}\end{cases} \tag{D1}$$

where $\overline{\overline{\epsilon}}$ is an electric permittivity tensor. If the permittivity tensor is anisotropic, then both the orbital and spin terms are in general nonzero. If the permittivity tensor is isotropic, the spin contribution is exactly 0 for all angles ϕ at each frequency ω while the orbital terms are in general nonzero.

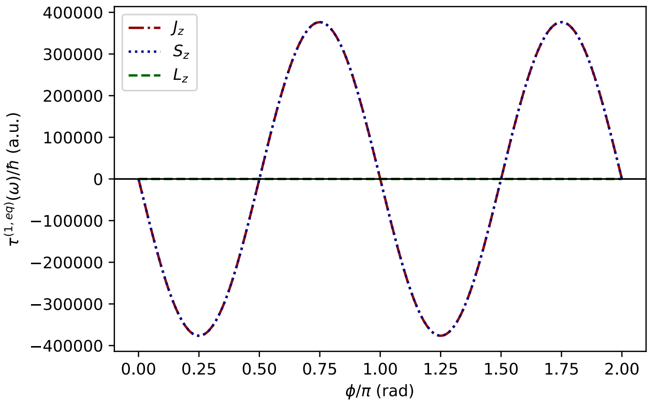

FIG. 4. Torque on the top particle (small sphere) as a function of angle ϕ of rotation with respective to a neighboring particle. Here $T = 300$ K, both particles have radius $R = 100$ nm, and the separation is $d = 1$ μm in the direction of the magnetic field.

Figure 3 shows the torque on the top wire as a function of the orientation ϕ between the wires as well as the magnitude and sign of the contributions of the $\hat{L}_z$ and $\hat{S}_z$ terms. Using finite-difference methods, we calculate $-\Delta\mathcal{F}_{J,L,S}/\Delta\phi$, where $\Delta\mathcal{F}_{J,L,S}$ is the change in free energy due to a slight geometric structure and dielectric rotation of the top wire (J) or solely geometric structure rotation (L) or solely from the dielectric matrix rotation (S), respectively. We also directly compute the torque using Eq. (C4) and plot the individual $\hat{L}_z$ and $\hat{S}_z$ contributions. The key takeaway is that the $\hat{S}$ contributions can be of the same order of magnitude as the $\hat{L}$ terms and can have the same or opposite sign.

For the case for which $\tau_{L_z} = 0$ but $\tau_{S_z} \neq 0$ perhaps the simplest example is that of two subthermal-wavelength balls (particles) which can be described by polarizability tensors $\overline{\overline{\alpha}}_1$ and $\overline{\overline{\alpha}}_2(\omega) \equiv 4\pi R_2^3 \frac{\overline{\overline{\epsilon}}_2(\omega)-\mathbb{I}}{\overline{\overline{\epsilon}}_2(\omega)+2\mathbb{I}}$ located a positions $\mathbf{r}_1$ and $\mathbf{r}_2$, respectively. In such a case, the torque expression reduces to Eq. (C5). We consider particles with permittivities

$$\overline{\overline{\epsilon}} = \begin{bmatrix} \epsilon_1 & -i\epsilon_2 & 0 \\ i\epsilon_2 & \epsilon_1 & 0 \\ 0 & 0 & \epsilon_3 \end{bmatrix}_{\text{cart}}. \tag{D2}$$

For InSb one has [54]

$$\epsilon_1 = \epsilon_\infty\left(1 + \frac{\omega_L^2 - \omega_T^2}{\omega_T^2 - \omega^2 - i\Gamma\omega} + \frac{\omega_p^2(\omega + i\gamma)}{\omega\left[\omega_c^2 - (\omega + i\gamma)^2\right]}\right), \tag{D3}$$

$$\epsilon_2 = \frac{\epsilon_\infty \omega_p^2 \omega_c}{\omega\left[(\omega + i\gamma)^2 - \omega_c^2\right]}, \tag{D4}$$

$$\epsilon_3 = \epsilon_\infty\left(1 + \frac{\omega_L^2 - \omega_T^2}{\omega_T^2 - \omega^2 - i\Gamma\omega} - \frac{\omega_p^2}{\omega(\omega + i\gamma)}\right), \tag{D5}$$

where $\epsilon_\infty = 15.7$, $\omega_L = 3.62 \times 10^{13}$ rad/s, $\omega_T = 3.39 \times 10^{13}$ rad/s, $n = 1.07 \times 10^{17}$ cm^{-3}, $m^* = 1.99 \times 10^{-32}$ kg, $\omega_p = \sqrt{\frac{nq^2}{m^*\epsilon_0\epsilon_\infty}} = 3.15 \times 10^{13}$ rad/s, $q = 1.6 \times 10^{-19}$ C, $\Gamma = 5.65 \times 10^{11}$ rad/s, $\gamma = 3.39 \times 10^{12}$ rad/s, and $\omega_c = \frac{eB}{m^*}$. See Fig. 4 for a plot of the torque contribution at a representative frequency.

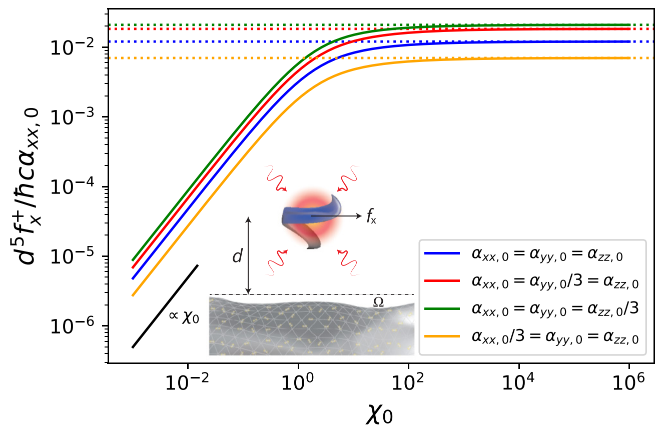

FIG. 5. Material dependence of bounds on Casimir force. Shown are upper bounds to the Casimir force at zero temperature in the surface-parallel direction on a nondispersive dipole above a half-space design domain Ω which contains a structure made of nondispersive susceptibility χ_0. As $\chi_0 \to \infty$, the bounds approach the perfect electrical conductor limit given by Eq. (F4), marked by horizontal dotted lines.

APPENDIX E: LINEAR RESPONSE AND FLUCTUATIONAL ELECTRODYNAMICS

Near equilibrium, linear response functions can be related to fluctuations of corresponding equilibrium quantities. This was verified to hold in the $\mathbb{T}$ operator trace formalism for fluctuational electrodynamics for heat transfer and forces in Ref. [55]. Using the newly derived trace expressions for equilibrium Casimir torque along with the nonequilibrium Casimir torque trace expressions from Ref. [13], we verified that, unsurprisingly, similar expressions hold for torque.

Let $H^{(\beta)}(t)$ denote the absorbed power by object β. It can be written as an integral over the volume V_β of the local power absorption, which is equal to the inner product of the electric field $\mathbf{E}(\mathbf{r}, t)$ and the current density $\mathbf{K}(\mathbf{r}, t)$,

$$H^{(\beta)}(t) = \int_{V_\beta} d^3\mathbf{r}\{E_a(\mathbf{r}, t), K_a(\mathbf{r}, t)\}_S, \tag{E1}$$

where we use the Einstein summation convention. Here $\{A, B\}_S \equiv (AB + BA)/2$ is the symmetrized product of two, in general, noncommuting operators.

A general operator $\hat{\Theta}^{(\beta)}(t)$ can be written as

$$\hat{\Theta}^{(\beta)}(t) \equiv \int_{\mathbf{r}\in V_\beta} d^3\mathbf{r} \int_{-\infty}^{\infty} d\omega \int_{-\infty}^{\infty} d\omega' e^{-i(\omega+\omega')t} \times \frac{1}{\hbar\omega}\{K_a(\mathbf{r}, \omega'), \hat{\Theta}E_a(\mathbf{r}, \omega)\}_S. \tag{E2}$$

We seek to evaluate

$$\int_0^\infty dt \langle\hat{\Theta}^{(\beta)}(t)H^{(\alpha)}(0)\rangle_{\text{eq}}, \tag{E3}$$

where H^α is as defined in Eq. (E1). Using Wick's theorem and simplifying, we find that Eq. (E3) is equal to

$$\int_0^\infty d\omega \int_{\mathbf{r}\in V_\beta}\int_{\mathbf{r}'\in V_\alpha}\frac{2\pi}{\hbar\omega}[\langle K_b(\mathbf{r})K_a^*(\mathbf{r}')\rangle_{-\omega}\langle\hat{\Theta}E_b(\mathbf{r})E_a^*(\mathbf{r}')\rangle_\omega + \langle K_b(\mathbf{r})E_a^*(\mathbf{r}')\rangle_{-\omega}\langle\hat{\Theta}E_b(\mathbf{r})K_a^*(\mathbf{r}')\rangle_\omega]. \tag{E4}$$

Note that $\int_0^\infty dt\,\langle\{A(t),B(0)\}_S\rangle_{\rm eq} = \int_0^\infty dt\,\langle A(t)B(0)\rangle_{\rm eq}$, so we now work with unsymmetrized correlators to reduce the number of terms from Wick's theorem by half. Using $\mathbf{E} = i\omega\mu_0\frac{c^2}{\omega^2}\mathbb{G}_0\mathbf{K}$ along with the unsymmetrical correlator [44]

$$\langle E_i(\mathbf{r},\omega)E_j^*(\mathbf{r}',\omega)\rangle_\omega = \frac{\hbar}{\pi\epsilon_0}\frac{1}{1-e^{-\frac{\hbar\omega}{k_BT}}}\mathbb{G}_{ij}^{\mathsf{A}}(\omega;\mathbf{r},\mathbf{r}'), \tag{E5}$$

we find

$$\int_0^\infty dt\,\langle\hat{\Theta}^{(\beta)}(t)H^{(\alpha)}(0)\rangle_{\rm eq} = \frac{2}{\pi}\int_0^\infty d\omega\frac{\hbar\omega e^{\hbar\omega/k_BT}}{(e^{\hbar\omega/k_BT}-1)^2}\big[\hat{\Theta}\mathbb{G}_{ba}^{\mathsf{A}}(\mathbf{r},\mathbf{r}')\mathbb{G}_{0,ad}^{-1}(\mathbf{r}',\mathbf{v})\mathbb{G}_{dc}^{\mathsf{A}}(\mathbf{v},\mathbf{u})\mathbb{G}_{0,cb}^{-1\dagger}(\mathbf{u},\mathbf{r})$$
$$-\hat{\Theta}\mathbb{G}_{bd}^{\mathsf{A}}(\mathbf{r},\mathbf{v})\mathbb{G}_{0,da}^{-1\dagger}(\mathbf{v},\mathbf{r}')\mathbb{G}_{ac}^{\mathsf{A}}(\mathbf{r}',\mathbf{u})\mathbb{G}_{0,cb}^{-1\dagger}(\mathbf{u},\mathbf{r})\big], \tag{E6}$$

where repeated indices are to be summed or integrated over. Integration is over all space except for $\mathbf{r}\in V_\beta$ and $\mathbf{r}'\in V_\alpha$.

Consider next a temperature perturbation; consider a change in $\boldsymbol{\tau}^{(\beta)}$, the torque on β, when all objects are at rest and at the same temperature but then the temperature of object α is perturbed to nonequilibrium. We find that

$$\left.\frac{d\langle\boldsymbol{\tau}^{(\beta)}\rangle_{\rm neq}}{dT_\alpha}\right|_{\{T_\alpha\}=T_{\rm eq}=T} = -\frac{1}{k_BT^2}\int_0^\infty dt\,\langle\boldsymbol{\tau}^{(\beta)}(t)H^{(\alpha)}(0)\rangle_{\rm eq}, \tag{E7}$$

confirming a relationship between variations in nonequilibrium torque and the equilibrium correlation of torque and power absorption. The equality is established by directly computing the right-hand side and comparing to a calculation of the left-hand side starting from the trace expression for nonequilibrium Casimir torque presented in Ref. [13]. Intermediate steps are outlined below. The explicit result of the correlation function in Eq. (E7) is provided in Eq. (E8). Using Eqs. (A5) and (A6) in Eq. (E6), we find

$$\int_0^\infty dt\,\langle\boldsymbol{\tau}^{(1)}(t)H^{(\alpha)}(0)\rangle_{\rm eq} = \frac{2}{\pi}\int_0^\infty d\omega\,\hbar\omega e^{\hbar\omega/k_BT}n(\omega,T)^2\,{\rm Im\,Tr}\big(\hat{\mathbf{J}}\mathbb{M}_\alpha^{(1)}\big), \tag{E8}$$

where

$$\mathbb{M}_1^{(1)} = (1+\mathbb{G}_0\mathbb{T}_2)\frac{1}{1-\mathbb{G}_0\mathbb{T}_1\mathbb{G}_0\mathbb{T}_2}\mathbb{G}_0\big(\mathbb{T}_1^{\mathsf{A}}-\mathbb{T}_1\mathbb{G}_0^{\mathsf{A}}\mathbb{T}_1^\dagger\big)\frac{1}{1-\mathbb{G}_0^\dagger\mathbb{T}_2^\dagger\mathbb{G}_0^\dagger\mathbb{T}_1^\dagger}, \tag{E9}$$

$$\mathbb{M}_2^{(1)} = (1+\mathbb{G}_0\mathbb{T}_1)\frac{1}{1-\mathbb{G}_0\mathbb{T}_2\mathbb{G}_0\mathbb{T}_1}\mathbb{G}_0\big(\mathbb{T}_2^{\mathsf{A}}-\mathbb{T}_2\mathbb{G}_0^{\mathsf{A}}\mathbb{T}_2^\dagger\big)\mathbb{G}_0^\dagger\frac{1}{1-\mathbb{T}_1^\dagger\mathbb{G}_0^\dagger\mathbb{T}_2^\dagger\mathbb{G}_0^\dagger}\mathbb{T}_1^\dagger. \tag{E10}$$

A key step is to note that $\mathbb{T}_{\alpha,ab}(\mathbf{u},\mathbf{v})$ vanishes if one of spatial arguments $\mathbf{u}$ or $\mathbf{v}$ is outside V_α, which eventually allows one to extend the integrals to be over all space, leading to a trace expression. The Casimir torque acting on an arbitrary object α is given by [13]

$$\langle\boldsymbol{\tau}^{(\alpha)}\rangle_{\rm neq}(T_{\rm eq},\{T_\beta\}) = \langle\boldsymbol{\tau}^{(\alpha)}\rangle_{\rm eq}(T_{\rm eq}) + \sum_\beta\big[\boldsymbol{\tau}_\beta^{(\alpha)}(T_\beta)-\boldsymbol{\tau}_\beta^{(\alpha)}(T_{\rm eq})\big], \tag{E11}$$

that is, the total Casimir torque in nonequilibrium can be written as a sum of an equilibrium contribution $\langle\boldsymbol{\tau}^{(\alpha)}\rangle_{\rm eq}(T_{\rm eq})$ where all objects are at a temperature $T_{\rm eq}$ plus nonequilibrium contributions when the objects $1,\ldots,N$ deviate from the temperature of the background environment $T_{\rm eq}$. Here $\boldsymbol{\tau}_\beta^{(\alpha)}(T)$ is the torque on α due to sources in β, when body β is at a temperature T. From Eqs. (23) and (24) in Ref. [13],

$$\boldsymbol{\tau}_{1,2}^{(1)}(T) = -\frac{2}{\pi}\int_0^\infty d\omega\,n(\omega,T)\,{\rm Im\,Tr}\big(\hat{\mathbf{J}}\mathbb{M}_{1,2}^{(1)}\big). \tag{E12}$$

From Eqs. (E11) and (E12) it follows that

$$\left.\frac{d\langle\boldsymbol{\tau}^{(1)}\rangle_{\rm neq}}{dT_\alpha}\right|_T = -\frac{2}{\pi k_BT^2}\int_0^\infty d\omega\,\hbar\omega e^{\hbar\omega/k_BT}n(\omega,T)^2\,{\rm Im\,Tr}\big(\hat{\mathbf{J}}\mathbb{M}_\alpha^{(1)}\big), \tag{E13}$$

which combined with Eq. (E8) proves Eq. (E7).

APPENDIX F: BOUNDS ON SURFACE-PARALLEL CASIMIR FORCES

In this Appendix we demonstrate how the derivation and discussion in the main text is also applicable to lateral forces. For example, expressions such as

$$\big(\hat{p}_x^2\mathbb{G}_{\text{sca}}\big)(i\xi, d\mathbf{e}_z, d\mathbf{e}_z) = \frac{\hbar^2}{2}\int_0^{2\pi}\int_0^\infty [k\cos(\psi)]^2[\mathbb{M}^{\text{s}}(i\xi,\mathbf{k}) + \mathbb{M}^{\text{p}}(i\xi,\mathbf{k})]e^{-2\kappa_z d}\frac{k\,dk\,d\psi}{(2\pi)^2} \tag{F1}$$

$$= \frac{\hbar^2}{128\pi d^5}\left[9 + 18\left(\frac{\xi d}{c}\right) + 16\left(\frac{\xi d}{c}\right)^2 + 8\left(\frac{\xi d}{c}\right)^3\right]\exp\left(-2\frac{\xi d}{c}\right)\begin{bmatrix}1&0&0\\0&0&0\\0&0&0\end{bmatrix}$$
$$+ \frac{\hbar^2}{128\pi d^5}\left[3 + 6\left(\frac{\xi d}{c}\right) + 8\left(\frac{\xi d}{c}\right)^2 + 8\left(\frac{\xi d}{c}\right)^3\right]\exp\left(-2\frac{\xi d}{c}\right)\begin{bmatrix}0&0&0\\0&1&0\\0&0&0\end{bmatrix}$$
$$+ \frac{\hbar^2}{32\pi d^5}\left[3 + 6\left(\frac{\xi d}{c}\right) + 4\left(\frac{\xi d}{c}\right)^2\right]\exp\left(-2\frac{\xi d}{c}\right)\begin{bmatrix}0&0&0\\0&0&0\\0&0&1\end{bmatrix} \tag{F2}$$

can also be used to derive bounds on lateral forces in the PEC limit on an anisotropic dipole above the half-space planar design domain. The expression for the bound on surface-parallel forces on a dipole above a half-space design domain in the PEC limit follows by, without loss of generality, setting $\hat{\Theta} = \hat{p}_x$, resulting in

$$f_{\text{dip},x}^{\pm,\text{PEC}}(T=0) = \pm\frac{\hbar c}{64\pi d^5}\int_0^\infty \alpha_{xx}\left(\frac{i\tilde{\xi}c}{d}\right)(9 + 36\tilde{\xi} + 88\tilde{\xi}^2 + 112\tilde{\xi}^3 + 80\tilde{\xi}^4 + 32\tilde{\xi}^5)^{1/2}e^{-2\tilde{\xi}}\frac{d\tilde{\xi}}{2\pi}$$
$$\pm\frac{\hbar c}{64\pi d^5}\int_0^\infty \alpha_{yy}\left(\frac{i\tilde{\xi}c}{d}\right)(3 + 12\tilde{\xi} + 32\tilde{\xi}^2 + 48\tilde{\xi}^3 + 48\tilde{\xi}^4 + 32\tilde{\xi}^5)^{1/2}e^{-2\tilde{\xi}}\frac{d\tilde{\xi}}{2\pi}$$
$$\pm\frac{\hbar c}{16\sqrt{2}\pi d^5}\int_0^\infty \alpha_{zz}\left(\frac{i\tilde{\xi}c}{d}\right)(3 + 12\tilde{\xi} + 16\tilde{\xi}^2 + 8\tilde{\xi}^3)^{1/2}e^{-2\tilde{\xi}}\frac{d\tilde{\xi}}{2\pi}. \tag{F3}$$

Assuming quasistatic polarizabilities of the dipole gives

$$f_{\text{dip},x}^{\pm,\text{PEC}}(T=0) = \pm\left(\frac{\hbar c}{128\pi^2 d^5}\gamma_{xx}\alpha_{xx,0} + \frac{\hbar c}{128\pi^2 d^5}\gamma_{yy}\alpha_{yy,0} + \frac{\hbar c}{32\sqrt{2}\pi^2 d^5}\gamma_{zz}\alpha_{zz,0}\right) \tag{F4}$$

$$\approx \pm\left(\frac{\hbar c}{128\pi^2 d^5}5.649\,58\alpha_{xx,0} + \frac{\hbar c}{128\pi^2 d^5}3.953\,99\alpha_{yy,0} + \frac{\hbar c}{32\sqrt{2}\pi^2 d^5}1.983\,09\alpha_{zz,0}\right), \tag{F5}$$

where

$$\gamma_{xx} \equiv \int_0^\infty (9 + 36\tilde{\xi} + 88\tilde{\xi}^2 + 112\tilde{\xi}^3 + 80\tilde{\xi}^4 + 32\tilde{\xi}^5)^{1/2}e^{-2\tilde{\xi}}d\tilde{\xi}, \tag{F6}$$

$$\gamma_{yy} \equiv \int_0^\infty (3 + 12\tilde{\xi} + 32\tilde{\xi}^2 + 48\tilde{\xi}^3 + 48\tilde{\xi}^4 + 32\tilde{\xi}^5)^{1/2}e^{-2\tilde{\xi}}d\tilde{\xi}, \tag{F7}$$

$$\gamma_{zz} \equiv \int_0^\infty (3 + 12\tilde{\xi} + 16\tilde{\xi}^2 + 8\tilde{\xi}^3)^{1/2}e^{-2\tilde{\xi}}d\tilde{\xi}. \tag{F8}$$

See Fig. 5 for a numerical evaluation of the bounds for finite nondispersive χ_0 and comparison (horizontal dotted lines) to the PEC limit given by Eq. (F4). For finite T, the expression for the bound on surface-parallel forces on a dipole above a half-space design domain in the PEC limit is

$$f_{\text{dip},x}^{\pm,\text{PEC}}(T>0) = \pm\frac{k_BT}{64\pi d^4}{\sum_{n=0}^{\infty}}'\alpha_{xx}(i\xi_n)\left[9 + 36\left(\frac{\xi_n d}{c}\right) + 88\left(\frac{\xi_n d}{c}\right)^2 + 112\left(\frac{\xi_n d}{c}\right)^3 + 80\left(\frac{\xi_n d}{c}\right)^4 + 32\left(\frac{\xi_n d}{c}\right)^5\right]^{1/2}e^{-2\xi_n d/c}$$
$$\pm\frac{k_BT}{64\pi d^4}{\sum_{n=0}^{\infty}}'\alpha_{yy}(i\xi_n)\left[3 + 12\left(\frac{\xi_n d}{c}\right) + 32\left(\frac{\xi_n d}{c}\right)^2 + 48\left(\frac{\xi_n d}{c}\right)^3 + 48\left(\frac{\xi_n d}{c}\right)^4 + 32\left(\frac{\xi_n d}{c}\right)^5\right]^{1/2}e^{-2\xi_n d/c}$$
$$\pm\frac{k_BT}{16\sqrt{2}\pi d^4}{\sum_{n=0}^{\infty}}'\alpha_{zz}(i\xi_n)\left[3 + 12\left(\frac{\xi_n d}{c}\right) + 16\left(\frac{\xi_n d}{c}\right)^2 + 8\left(\frac{\xi_n d}{c}\right)^3\right]^{1/2}e^{-2\xi_n d/c}, \tag{F9}$$

where $\xi_n = 2\pi k_{\text{B}}Tn/\hbar$ and the prime on the summation implies a prefactor of $\frac{1}{2}$ for the contribution at $n = 0$.

[1] G. L. Klimchitskaya, U. Mohideen, and V. M. Mostepanenko, The Casimir force between real materials: Experiment and theory, Rev. Mod. Phys. **81**, 1827 (2009).

[2] L. M. Woods, D. A. R. Dalvit, A. Tkatchenko, P. Rodriguez-Lopez, A. W. Rodriguez, and R. Podgornik, Materials perspective on Casimir and van der Waals interactions, Rev. Mod. Phys. **88**, 045003 (2016).

[3] E. Rousseau, A. Siria, G. Jourdan, S. Volz, F. Comin, J. Chevrier, and J.-J. Greffet, Radiative heat transfer at the nanoscale, Nat. Photon. **3**, 514 (2009).

[4] J. C. Cuevas and F. J. García-Vidal, Radiative heat transfer, ACS Photon. **5**, 3896 (2018).

[5] S. K. Lamoreaux, Demonstration of the Casimir force in the 0.6 to 6 μm range, Phys. Rev. Lett. **78**, 5 (1997).

[6] U. Mohideen and A. Roy, Precision measurement of the Casimir force from 0.1 to 0.9 μm, Phys. Rev. Lett. **81**, 4549 (1998).

[7] J. N. Munday, F. Capasso, and V. A. Parsegian, Measured long-range repulsive Casimir–Lifshitz forces, Nature (London) **457**, 170 (2009).

[8] E. I. Kats, Van der Waals forces in non-isotropic systems, Zh. Eksp. Teor. Fiz. **60**, 1172 (1971) [Sov. Phys. JETP **33**, 634 (1971)].

[9] V. A. Parsegian and G. H. Weiss, Dielectric anisotropy and the van der Waals interaction between bulk media, J. Adhesion **3**, 259 (1972).

[10] C. Khandekar, S. Buddhiraju, P. R. Wilkinson, J. K. Gimzewski, A. W. Rodriguez, C. Chase, and S. Fan, Nonequilibrium lateral force and torque by thermally excited nonreciprocal surface electromagnetic waves, Phys. Rev. B **104**, 245433 (2021).

[11] Y. Guo and S. Fan, Single gyrotropic particle as a heat engine, ACS Photon. **8**, 1623 (2021).

[12] X. Gao, C. Khandekar, Z. Jacob, and T. Li, Thermal equilibrium spin torque: Near-field radiative angular momentum transfer in magneto-optical media, Phys. Rev. B **103**, 125424 (2021).

[13] B. Strekha, S. Molesky, P. Chao, M. Krüger, and A. W. Rodriguez, Trace expressions and associated limits for nonequilibrium Casimir torque, Phys. Rev. A **106**, 042222 (2022).

[14] J. N. Munday, D. Iannuzzi, Y. Barash, and F. Capasso, Torque on birefringent plates induced by quantum fluctuations, Phys. Rev. A **71**, 042102 (2005).

[15] R. B. Rodrigues, P. A. M. Neto, A. Lambrecht, and S. Reynaud, Vacuum-induced torque between corrugated metallic plates, Europhys. Lett. **76**, 822 (2006).

[16] R. Guérout, C. Genet, A. Lambrecht, and S. Reynaud, Casimir torque between nanostructured plates, Europhys. Lett. **111**, 44001 (2015).

[17] D. A. T. Somers and J. N. Munday, Rotation of a liquid crystal by the Casimir torque, Phys. Rev. A **91**, 032520 (2015).

[18] D. A. T. Somers, J. L. Garrett, K. J. Palm, and J. N. Munday, Measurement of the Casimir torque, Nature (London) **564**, 386 (2018).

[19] Z. Xu and T. Li, Detecting Casimir torque with an optically levitated nanorod, Phys. Rev. A **96**, 033843 (2017).

[20] J. Ahn, Z. Xu, J. Bang, Y.-H. Deng, T. M. Hoang, Q. Han, R.-M. Ma, and T. Li, Optically levitated nanodumbbell torsion balance and GHz nanomechanical rotor, Phys. Rev. Lett. **121**, 033603 (2018).

[21] J. Ahn, Z. Xu, J. Bang, P. Ju, X. Gao, and T. Li, Ultrasensitive torque detection with an optically levitated nanorotor, Nat. Nanotechnol. **15**, 89 (2020).

[22] S. J. Rahi, T. Emig, N. Graham, R. L. Jaffe, and M. Kardar, Scattering theory approach to electrodynamic Casimir forces, Phys. Rev. D **80**, 085021 (2009).

[23] T. Emig, N. Graham, R. L. Jaffe, and M. Kardar, Casimir forces between arbitrary compact objects, Phys. Rev. Lett. **99**, 170403 (2007).

[24] D. Gelbwaser-Klimovsky, N. Graham, M. Kardar, and M. Krüger, Equilibrium forces on nonreciprocal materials, Phys. Rev. B **106**, 115106 (2022).

[25] S. M. Rytov, Y. A. Kravtsov, and V. I. Tatarskii, *Principles of Statistical Radiophysics: Elements of Random Fields* (Springer, Berlin, 1989).

[26] C. R. Otey, L. Zhu, S. Sandhu, and S. Fan, Fluctuational electrodynamics calculations of near-field heat transfer in non-planar geometries: A brief overview, J. Quant. Spectrosc. Radiat. Transfer **132**, 3 (2014).

[27] M. Antezza, H. B. Chan, B. Guizal, V. N. Marachevsky, R. Messina, and M. Wang, Giant Casimir torque between rotated gratings and the $\theta = 0$ anomaly, Phys. Rev. Lett. **124**, 013903 (2020).

[28] H. Ding, P. S. Kollipara, Y. Kim, A. Kotnala, J. Li, Z. Chen, and Y. Zheng, Universal optothermal micro/nanoscale rotors, Sci. Adv. **8**, eabn8498 (2022).

[29] F. van der Laan, F. Tebbenjohanns, R. Reimann, J. Vijayan, L. Novotny, and M. Frimmer, Sub-Kelvin feedback cooling and heating dynamics of an optically levitated librator, Phys. Rev. Lett. **127**, 123605 (2021).

[30] B. A. Stickler, K. Hornberger, and M. S. Kim, Quantum rotations of nanoparticles, Nat. Rev. Phys. **3**, 589 (2021).

[31] S. Molesky, Z. Lin, A. Y. Piggott, W. Jin, J. Vucković, and A. W. Rodriguez, Inverse design in nanophotonics, Nat. Photon. **12**, 659 (2018).

[32] R. E. Christiansen and O. Sigmund, Inverse design in photonics by topology optimization: Tutorial, J. Opt. Soc. Am. B **38**, 496 (2021).

[33] S. Molesky, W. Jin, P. S. Venkataram, and A. W. Rodriguez, $\mathbb{T}$ operator bounds on angle-integrated absorption and thermal radiation for arbitrary objects, Phys. Rev. Lett. **123**, 257401 (2019).

[34] S. Molesky, P. Chao, W. Jin, and A. W. Rodriguez, Global $\mathbb{T}$ operator bounds on electromagnetic scattering: Upper bounds on far-field cross sections, Phys. Rev. Res. **2**, 033172 (2020).

[35] P. Chao, B. Strekha, R. K. Defo, S. Molesky, and A. W. Rodriguez, Physical limits in electromagnetism, Nat. Rev. Phys. **4**, 543 (2022).

[36] P. S. Venkataram, S. Molesky, P. Chao, and A. W. Rodriguez, Fundamental limits to attractive and repulsive Casimir-Polder forces, Phys. Rev. A **101**, 052115 (2020).

[37] B. Strekha, P. Chao, R. K. Defo, S. Molesky, and A. W. Rodriguez, Suppressing electromagnetic local density of states via slow light in lossy quasi-1d gratings, arXiv:2309.15794.

[38] M. Krüger, G. Bimonte, T. Emig, and M. Kardar, Trace formulas for nonequilibrium Casimir interactions, heat radiation, and heat transfer for arbitrary objects, Phys. Rev. B **86**, 115423 (2012).

[39] Y.-M. Zhang, T. Zhu, Z.-Q. Zhang, and J.-S. Wang, Microscopic theory of photon-induced energy, momentum, and angular momentum transport in the nonequilibrium regime, Phys. Rev. B **105**, 205421 (2022).

[40] J.-S. Wang, J. Peng, Z.-Q. Zhang, Y.-M. Zhang, and T. Zhu, Transport in electron-photon systems, Front. Phys. **18**, 43602 (2023).

[41] J.-S. Wang and M. Antezza, Photon mediated energy, linear and angular momentum transport in fullerene and graphene systems beyond local equilibrium, arXiv:2307.11361.

[42] V. K. Khersonskii, A. N. Moskalev, and D. A. Varshalovich, *Quantum Theory Of Angular Momemtum* (World Scientific, Singapore, 1989).

[43] G. Bimonte, T. Emig, M. Kardar, and M. Krüger, Nonequilibrium fluctuational quantum electrodynamics: Heat radiation, heat transfer, and force, Annu. Rev. Condens. Matter Phys. **8**, 119 (2017).

[44] L. Novotny and B. Hecht, *Principles of Nano-Optics* (Cambridge University Press, Cambridge, 2012).

[45] S. Boyd and L. Vandenberghe, *Convex Optimization* (Cambridge University Press, Cambridge, 2004).

[46] J. D. Jackson, *Classical Electrodynamics* (Wiley, New York, 1999).

[47] S. Molesky, P. Chao, and A. W. Rodriguez, Hierarchical mean-field $\mathbb{T}$ operator bounds on electromagnetic scattering: Upper bounds on near-field radiative Purcell enhancement, Phys. Rev. Res. **2**, 043398 (2020).

[48] A. Amaolo, P. Chao, T. J. Maldonado, S. Molesky, and A. W. Rodriguez, Can photonic heterostructures provably outperform single-material geometries? arXiv:2307.00629.

[49] G. Angeris, J. Vučković, and S. P. Boyd, Computational bounds for photonic design, ACS Photon. **6**, 1232 (2019).

[50] H. Shim, L. Fan, S. G. Johnson, and O. D. Miller, Fundamental limits to near-field optical response over any bandwidth, Phys. Rev. X **9**, 011043 (2019).

[51] P. S. Venkataram, S. Molesky, W. Jin, and A. W. Rodriguez, Fundamental limits to radiative heat transfer: The limited role of nanostructuring in the near-field, Phys. Rev. Lett. **124**, 013904 (2020).

[52] W. Eckhardt, Macroscopic theory of electromagnetic fluctuations and stationary radiative heat transfer, Phys. Rev. A **29**, 1991 (1984).

[53] K. Asheichyk, B. Müller, and M. Krüger, Heat radiation and transfer for point particles in arbitrary geometries, Phys. Rev. B **96**, 155402 (2017).

[54] A. Ott, R. Messina, P. Ben-Abdallah, and S.-A. Biehs, Magnetothermoplasmonics: From theory to applications, J. Photon. Energy **9**, 032711 (2019).

[55] V. A. Golyk, M. Krüger, and M. Kardar, Linear response relations in fluctuational electrodynamics, Phys. Rev. B **88**, 155117 (2013).